Copyright Warning & Restrictions

The copyright law of the United States (Title 17, United States Code) governs the making of photocopies or other reproductions of copyrighted material.

Under certain conditions specified in the law, libraries and archives are authorized to furnish a photocopy or other reproduction. One of these specified conditions is that the photocopy or reproduction is not to be "used for any purpose other than private study, scholarship, or research." If a, user makes a request for, or later uses, a photocopy or reproduction for purposes in excess of "fair use" that user may be liable for copyright infringement,

This institution reserves the right to refuse to accept a copying order if, in its judgment, fulfillment of the order would involve violation of copyright law.

Please Note: The author retains the copyright while the New Jersey Institute of Technology reserves the right to distribute this thesis or dissertation

Printing note: If you do not wish to print this page, then select "Pages from: first page # to: last page #" on the print dialog screen

ABSTRACT

CAD STUDY OF LINEAR TAPERED SLOT ANTENNA

by
Anthony W. Kwan

Linear Tapered Slot Antenna (LTSA) is an attractive candidate as a radiating element in frequency scanning arrays. LTSA element backed by a rectangular cavity had been investigated and is proven to posses various physical design parameters suitable to optimize its performance. This study is focused on the feed position variation to optimize the performance while maximum of the current density variation is maintained in the slot region. It was observed that if the stub base of the microstrip feed structure is located in the middle of the slot region, current maximum can be obtained within the slot region at the expense of smaller return loss, contrary to the previously obtained optimization where the base of the stub was on the side of the slot line region.

Furthermore, if the rectangular cavity is replaced by a circular cavity, then there is a slight increase in the bandwidth and a small drop in the return loss. When two LTSA elements are placed back to back and excitation is achieved via strip line, rather than a single element microstrip excitation, circular cavity backed radiating elements could be tuned to obtain higher return loss. The strip line excitation also caused the decrease in the bandwidth. The mode structure excited in the circular cavity has to be studied further as well as its effects of the resonance frequency of the LTSA.

CAD STUDY OF LINEAR TAPERED SLOT ANTENNA

by
Anthony W. Kwan

A Thesis
Submitted to the Faculty of
New Jersey Institute of Technology
in Partial Fulfillment of the Requirements for the Degree of
Master of Science in Electrical Engineering

Department of Electrical and Computer Engineering

October 1994

APPROVAL PAGE

CAD STUDY OF LINEAR TAPERED SLOT ANTENNA

Anthony W. Kwan

Dr. Edip Niver, Thesis Advisor — Date
Associate Professor of Electrical Engineering,
New Jersey Institute of Technology

Dr. Gerald Whitman, Committee Member — Date
Professor of Electrical Engineering,
New Jersey Institute of Technology

Dr. Gary Wu, Committee Member — Date
Assistant Professor of Electrical Engineering,
New Jersey Institute of Technology

BIOGRAPHICAL SKETCH

Author: Anthony W. Kwan

Degree: Master of Science in Electrical Engineering

Date: October, 1994

Graduate and Undergraduate Education:

-Master of Science in Electrical Engineering
New Jersey Institute of Technology, Newark, NJ, 1994

-Bachelor of Science in Electrical Engineering
New Jersey Institute of Technology, Newark, NJ, 1986

Major: Electrical Engineering

ACKNOWLEDGMENT

The author wishes to gratefully express his sincere gratitude to Dr. Edip Niver for showing his continue support, tremendous amount of patience and ideas over the years which made this research possible. Dr. Robert T. Kinasewitz's (Picatinny Arsenal, US Army) suggestion of the problem and support, and Mr. Mark Bates' (Fort Monmouth, US Army) guidance and assistance in technical aspects are gratefully acknowledged.

The author also wishes to thank Lisa Lee, his wife, for all the patience and support she had offered over the entire time.

The same goes to Mr. Yung Kwan, his father, and Mrs. Wai-Han Chan, his mother, for all their support both morally and financially.

TABLE OF CONTENTS

LIST OF TABLES

LIST OF FIGURES

Figure Page

CHAPTER 1

INTRODUCTION

The growing number of applications, both in commercial and military sectors, require antenna array usage at microwave and millimeter wavelengths. The improved electrical performance measurable in terms of gain, beamwidth, side lobe level and bandwidth has to be complemented by physical properties such as low profile, light weight, ease of manufacturability and reduced cost. Conventional phase arrays are prohibitively expensive for most commercial applications. Emerging technologies, e.g. Intelligent Vehicle Highway System, etc., are considering anti-collision radars at 77 GHz, in motor vehicles, such applications would require low cost antenna systems. The key in these applications is to produce antenna systems in high volume at low cost without sacrificing the electrical performance.

Integrated antennas [1] where radiating elements and associated feed networks (sometimes complemented with active elements) are currently being considered as an attractive solution to these challenging problems. A good survey can be found in open literature on such integrated antenna structures [1].

Conventional phase array topologies require phase shifting capability in addition to radiating elements and the associated feed network at microwave and millimeter wave frequencies. Phase shifters (solid state, ferrite, etc.) are becoming limiting elements which influence physical parameters such as cost, bandwidth, weight, etc. An attractive

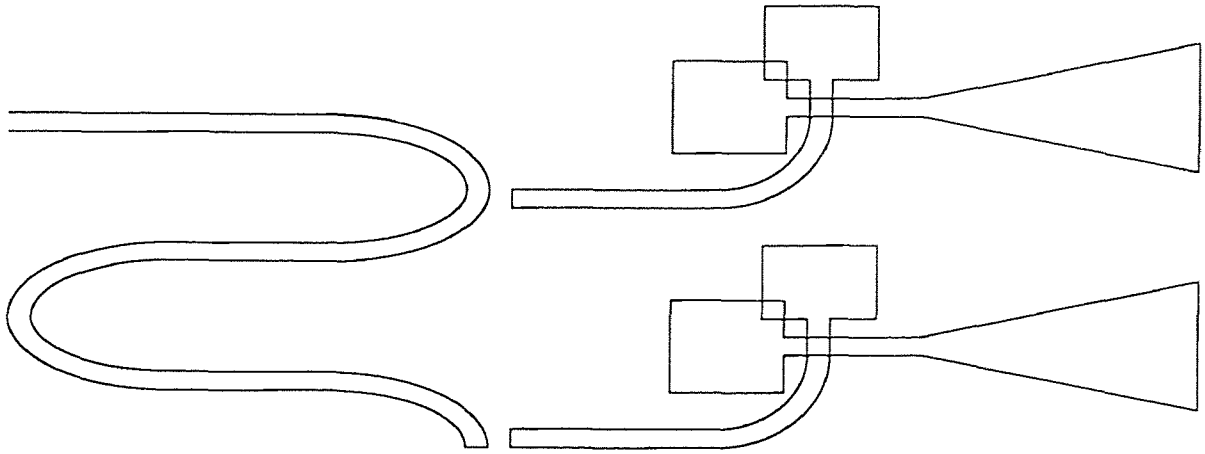

(a) Planar view of the 2 element array.

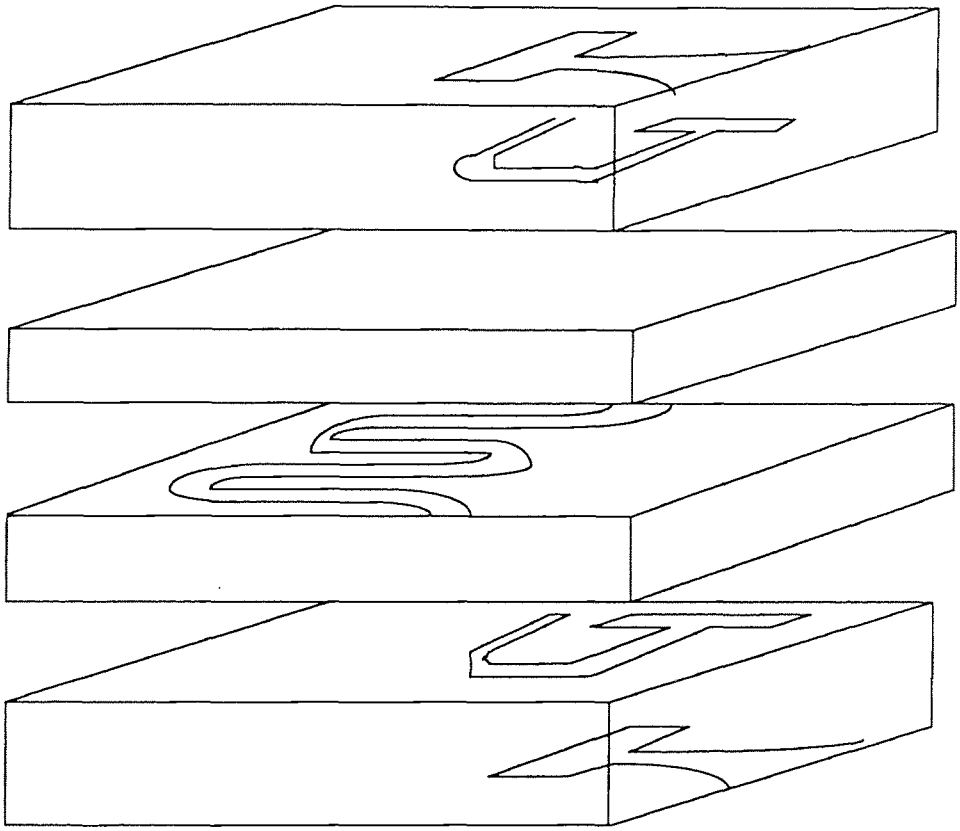

(b) 3 Dimensional representation of the array.

Figure 1. Various views of a Linear Tapered Slot Antenna (LTSA) array.

cost effective alternative to minimize this limitation is to use frequency scanning arrays. In this work, radiating element of such frequency scanning arrays comprised of Linear Tapered Slot Antenna (LTSA) fed by strip lines only is considered (see Figure 1).

Frequency scanning [2] antenna is a radiating structure in which the direction of the radiating beam is controlled by changing the operating frequency. Simplicity, reliability and low cost are virtues of frequency scan. More updated information can be found in the literature [3].

The meander line used in the feed network provides a possibility to obtain sufficient phase difference between radiating elements. The detailed analysis of meander lines can be found literature [4]. The physical distance " s " in Figure 2 has an electrical length [s`] which depends on the frequency, sufficient enough to provide adequate phase shift to excite radiating elements with the proper phase.

The couplers on the microstrip substrate have been reported extensively in the open literature [5].

In this work, the detailed CAD analysis of the radiating element will be investigated. The radiating element consisting of a notch antenna is coupled to a resonance cavity which is excited through coupling to a strip line will be thoroughly discussed in Chapter 2.

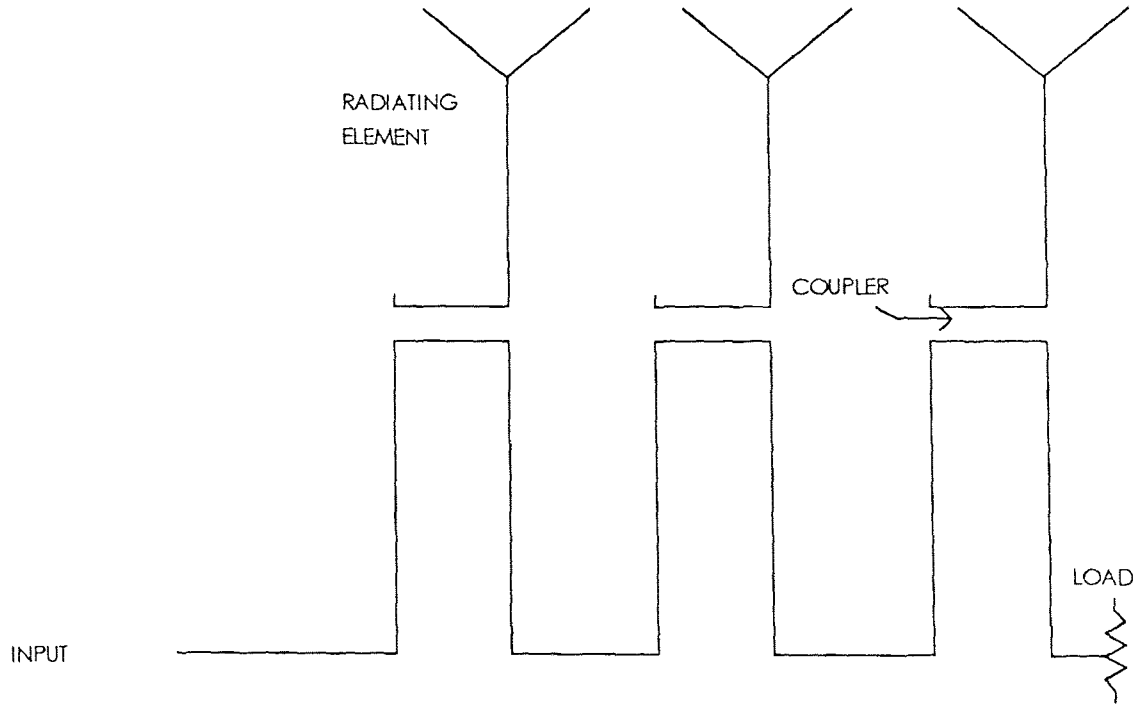

Figure 2. Linear array feed.

CHAPTER 2

RADIATING ELEMENT OF FREQUENCY SCAN : TAPERED SLOT ANTENNA

A detailed explanation of the radiating element for frequency scanning arrays have been presented below. Comparisons in terms of advantages and disadvantages for various geometries of these radiating elements are included. Antenna feed structures relevant to this study have also been discussed below.

2.1 Radiating element: Tapered slot antenna

The radiating element considered in this work has to have certain unique features:

- part of an integrated antenna structure (meander feed networks),
- ease of fabrication,
- low cost,
- meet the electrical performance specifications.

The slot line antenna [6,7] meets the desired features outlined above and can easily be fabricated with traditional methods and is cost effective. " Vivaldi " antenna shown in Figure 3 was first introduced by Gibson [6] and it consists of a metalized dielectricsubstrate with an exponential slot in the metalization. The variations of this original " Vivaldi " configuration are [8]

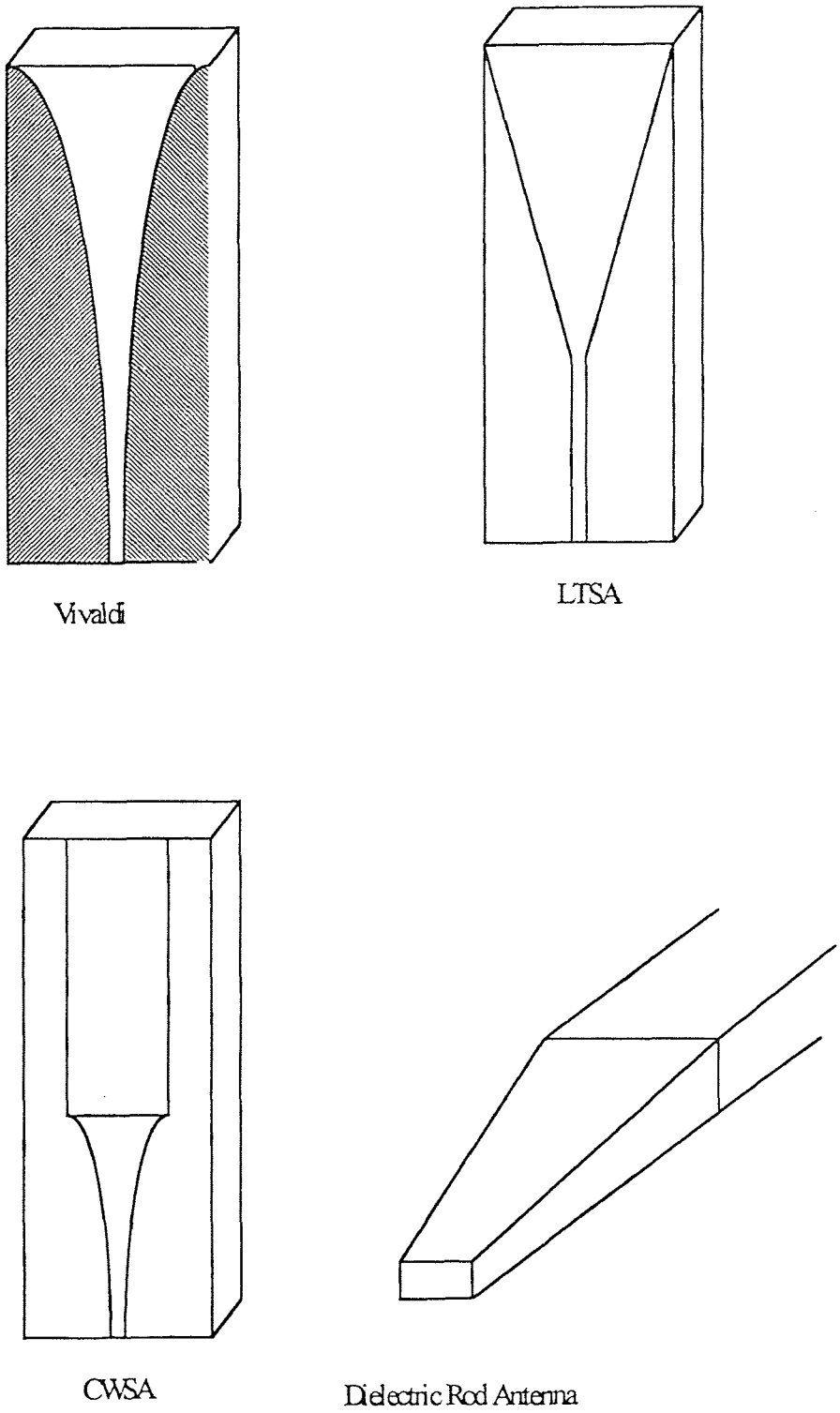

Figure 3. The three common types of endfire tapered slot antennas and a dielectric antenna

- Linear Taper Slot Antenna (LTSA)

- Constant Width Slot Antenna (CWSA)

As seen in Figure 3, they all resemble a dielectric rod antenna, but slot antennas have certain advantages.

One of the most distinguished characteristics of a tapered slot antenna is its ability of producing a symmetric beam (in E- and H- plane) over a wide band of frequencies in spite of their planar geometry. However, the necessary condition is that parameters such as shape, total length, dielectric thickness and dielectric constant have to be chosen carefully and this simply is not an easy task. Influence of these parameters is being outlined in the following sections, and tapered slot antennas are generally classified as traveling wave antennas and have moderate gain and highly low profile. Two main types of traveling wave antennas are "Leaky Wave Antenna "and "Surface Wave Antenna "[8]. The first type is based on the principle that leaky wave arises when either a closed or open waveguide structure supporting a guided wave is perturbed. The traveling wave propagating along the waveguide structure typically has a phase velocity $v_{ph} > c$. The main beam also occurs in a direction other than end-fire. Surface wave antenna, is quite the opposite, with the phase velocity $v_{ph} < c$ or $v_{ph} = c$ in the limiting case and it produces endfire radiation instead. Since endfire radiation is what being of interest here, and the following discussion is restricted to surface wave antennas.

Surface wave antennas are generally very flat due to their thin substrate. Typically gain of these type of antenna do not exceed 20 dB and their bandwidth is usually narrow.

Maximum gain of the antenna can be obtained if the Hansen-Woodyard [8] condition ($G = 7L/\lambda$) is met provided that it is very long (length $L >> \lambda$). If Ehrenspeck-Poehler conditions (equation 12.14 in [8]) are met, arbitrary length antenna can also reach the optimum gain condition. The directivity D typically has the ratio of $10L/\lambda_o$ with the length L, $3\lambda_o < L < 8\lambda_o$.. This criteria is common to most end-fire traveling wave antennas. All antennas discussed in this work have tapered width and the resulting phase velocity is not constant along the antenna, and hence the propagation constant becomes complex due to radiation losses. Zucker [9] determined the optimum gain and beamwidth of such antennas. These results are shown in Figure 4 and are often viewed as " standard data " for comparison. By comparing with the " standard data ", conclusions can usually be drawn whether a design represents a "well behaved and optimized " traveling antenna. A practical antenna has to be close to the optimum curve over a wide range of normalized length.

The exponential geometry of the Vivaldi antenna closely follows:

$$y(x) = +Ae^{px}$$

The opening angle α unlike the linear taper slot antenna (LTSA) which will be discussed in the next section, has a very large effect on the performance both on the beamwidth and gain of the antenna. If the antenna is sufficiently long with this linear taper, frequency independence can basically be achieved. The operating principle can be viewed at a given wavelength where only one section of the exponential taper is radiating efficiently. At a different wavelength, the radiation will occur at another section which is scaled in size proportional to the wavelength which has the same relative ratio. Such antenna is very easy

to design if the beamwidth does not have to be very narrow, an ultra wide band can be achieved. Gibson [1] has already proved these aspects in his original design. The beamwidth of his design was ranging 30° to 45° over the frequency range of 3.25:1 with a usable beamwidth over a 5:1 range. Gibson also allowed the exponential of the antenna opened up rapidly. This effectively made the effective radiating length much shorter than the physical length. The results of his antenna again emphasized on frequency independence rather than maximum gain for a given length. Vivaldi antenna with narrow beam and not ultrawide beamwidth can be easily achieved and was successfully designed on duroid substrate [8] at 10 and 25 GHz.

Linear taper slot antenna (LTSA) was first introduced by Prasad and Mahapatra [7]. Their antenna is etched on a Alumina substrate with the length approximately equal to λ and is considered to be short. Attempts [10] have been made to simplify the LTSA with air substrate (ε_r =1) to a V-shape antenna model with two line sources separated at an angle α. But the calculated beamwidth and beamshapes were quite different with the measured data of the LTSA. Carrell [11] who utilized a fin-antenna model and conformal mapping to find the impedance and field distribution obtained more satisfactory performance. A generalized statement can be made that the beamwidth of LTSA with air substrate follows the $1 / \sqrt{L / \lambda}$ relationship and this type of antenna does not have an optimal gain since $c/v_{ph} = 1$. A reasonable conclusion can also be drawn that the beamwidths are wider than the ones in Zucker's Standard Curve in Figure 4 (a) and Figure 4 (b).

If the substrate of the LTSA is anything but air (ε_r =1), according to the general theory of traveling wave antennas, there should exist a dielectric with dielectric constant for which c/v_{ph} has a value that will yield optimum gain. Indeed, Yngvesson [8] had carried out numerous experiments with different dielectrics at a fixed frequency. He was able to obtain optimum gain over a wide range of normalized lengths. The beamwidths were also bounded by the Zucker's " Standard curve ". There is one very interesting observation that he made that is different from the expected performance based on Vivaldi antenna (exponential taper). The beamwidth remained unchanged even for angular variation of α, $11.2^\circ < \alpha < 19.4^\circ$. This is a big contrast, when one compares Vivaldi antenna which is rather sensitive to the opening angle α and observed drastically performance results due to variations in an opening angle α.

The comparison of various widths of different substrates by Yngvesson are summarized in Table 1. This data turns out to be a very useful reference for the material selection process in the current application. Yngvesson's experimental data confirms that LTSA with thin substrate and low dielectric constant can produce beamwidth which fall within the optimum bounds in Zucker's " Standard Curve " especially for the " low-side lobes " case. For the thicker substrate case, the E-plane beamwidth becomes very steep and the H-plane remains relatively unchanged. It also follows very closely the " high gain " case rather than " low-sidelobes " in Zucker's " Standard Curve " .

3 dB Beamwidth

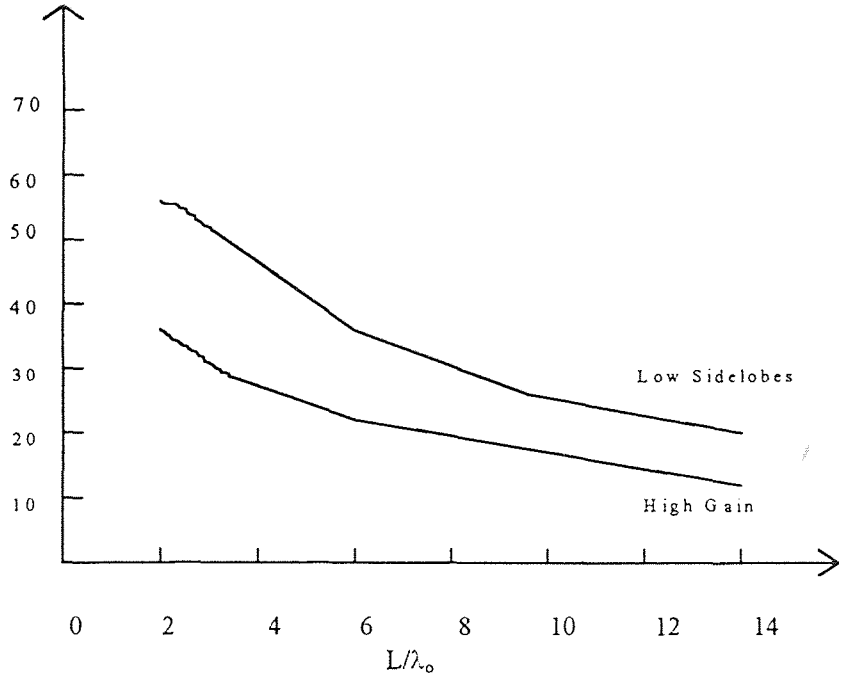

(a) H-plane

3 dB Beamwidth

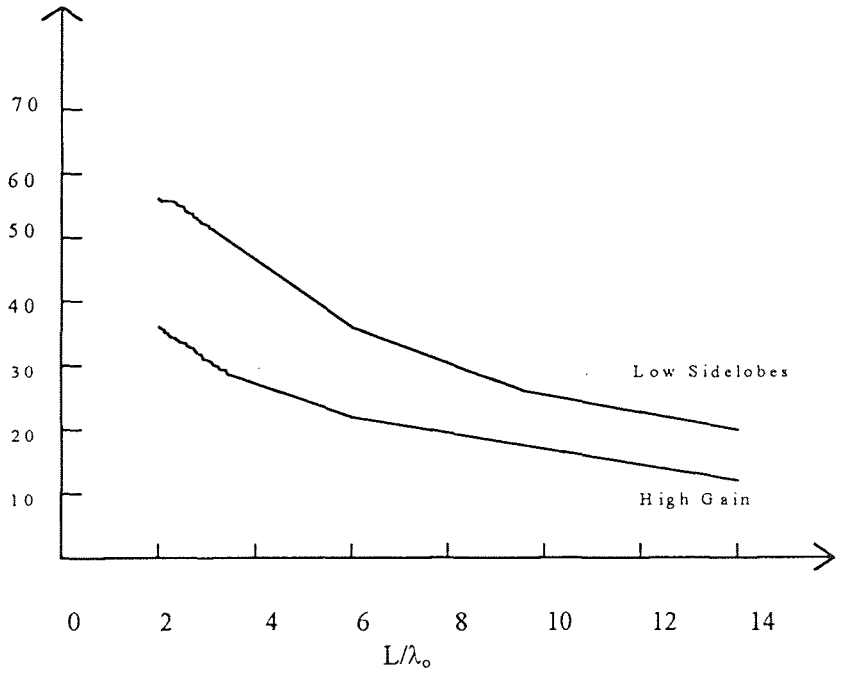

(b) E-plane

Figure 4. E-plane and H-plane of Zucker's standard curves.

An easy way of designing a LTSA to a desirable response can be done by choosing the effective dielectric thickness (t_{eff}). The following equation is normalized with respect to λ_o for convenience.

$$t_{eff} / \lambda_o = (\sqrt{\varepsilon_r} - 1)t / \lambda_o$$

The smaller the value of t_{eff}, the greater resemblance to the traveling wave behavior. With increasing t_{eff} the antenna will exhibit higher gain behavior. The antenna will eventually have asymmetric beams in the E-plane and H-plane when the substrate

TABLE 1 Comparisons of different characteristics of 3 different substrate from thin to thick[8]

Material	ε_r	Effective Thickness (mils)	Traveling-Wave Properties
Duroid	2.33	0.0025	Low sidelobes
Duroid	2.33	0.023	High gain
Duroid	2.33	0.026	Asymmetric E/H plane
Duroid	2.33	0.028	Asymmetric E/H plane High gain
Kapton	3.5	0.025	Low sidelobes
Kapton	3.5	0.05	High gain
Kapton	3.5	0.076	Asymmetric E/H plane
Epsilam	10.0	0.018	Asymmetric E/H plane

becomes very thick. E-plane and H-plane patterns also behave quite differently over the length of the antenna. Both plane beamwidths increase very fast when length is below $5\lambda_o$, but E-plane beamwidth stays constant while H-plane beamwidth continues to increase at longer lengths. One final observation from Yngvesson's data is cutoff wavelength can be defined as

$$\lambda_c = 2W$$

where W is the aperture size of the antenna, As W approaches $\lambda/2$, the antenna no longer can act as a traveling antenna.

Quasi-static techniques have been used [11] in the past to predict impedance of the LTSA and experimental data in Yngvesson [8] seem to track these calculations very well. The impedance basically goes up as the angle of the taper widens. One important conclusion can be drawn from this comparison is that impedance with thin dielectric can stay relatively frequency independent.

Constant Width Slot Antenna (CWSA) always requires some kind of taper (usually exponential) to feed the radiating element. Length of the feed taper mostly depends on the width of the slot. The E-plane beamwidth of the CWSA is usually very wide and it decreases quite rapidly with the increase in slot length. Since the wave traveling down the slot is bounded, the traveling wave radiation is suppressed. The optimum of the phase delay can be reached in approximately 5 to 6 times of λ_o. The side lobes will grow rapidly and the main beam will split if the CWSA length goes beyond this ratio. The antenna becomes practically useless at this point.

Dielectric rod antenna is a good directional radiator in the end-fire direction [12]. Zucker's principle [9] is applicable if maximum gain of the antenna is desired. According to Zucker's observations, radiation from the surface-wave structure takes place at the discontinuities (e.g. feed and terminal point). He also pointed out that radiation pattern due to the discontinuities at the termination can be calculated by integrating over the terminal aperture S_t which can be approximately expressed as $1/\psi$ where

$$\psi = 1/2\ k_o L(r - \cos\theta)$$

where $r = k_r / k_o$, k_z is a wave number in a dielectric in z-direction, k_o is the free space wave number, and L is the length of the antenna.

Interestingly enough this type of antenna exhibits similar behavior as the CWSA when the length of the antenna goes beyond the optimum phase delay. As it is being verified in experiment by Kobayashi[12] , the gain of the antenna becomes very low and the sidelobes of the antenna become as large as the main beam. The main beam in most case is split as in the case of the CWSA. The possible reasons of this type of behavior are :

- a degradation of the transition section,

- the local wavelength in the direction of the rod at the feed end is too large to satisfy the phase difference condition which prescribes for very short length of the rod.

Longer length rod just simply violates the phase difference which leads to low gain and distorted main beam. A comparison of the four types of traveling wave antennas is summarized in Table 2. One observation from the Yngvesson [8] radiation pattern suggests that there exits deep null outside the main beam in the E-plane. However, this does not

exist in the Vivaldi antenna and the curvature of the antenna basically fills the null. The sidelobes of both Vivaldi and LTSA has rather high sidelobes as compared to other types of feed antenna and they do not have high enough efficiency for applications such as illuminating a large reflector. From the calculations of Yngvesson [8] the height of the sidelobes typically are proportional to the length of the antenna.

As far as directivity is concerned, the CWSA's beam characteristics seems to fall within the high gain part of the Zucker's " Standard Curve " which yields the best result. LTSA, Vivaldi and dielectric rod, all fall in the low sidelobes side of Zucker's " standard curve " .

TABLE 1 Comparisons of different characteristics of 3 different substrate from thin to thick[8]

	Antenna Type	Characteristics
1)	Vivaldi (Exponential)	Low cross polarized radiation, wide-band antenna, length, height and rate of openings (three design parameters)
2)	Linear (LTSA)	Higher cross polarized radiation, (compared to exponential type) easy to design and etch, length and width or opening angle, (2 design parameters)
3)	Constant width (CWSA)	Better control of radiation pattern, taper section is mandatory as a transition from narrow feed to straight beam-forming section, many design parameters.
4)	Dielectric rod antenna	Good directional radiator, low gain, many design parameters.

2.2 Excitation of a tapered slot antenna

In any radiating structure, the radiating fields are excited through a proper connection of a suitable source. However, the rigorous solution to the boundary value problem of the radiating element and the source is difficult to obtain. Fortunately, with certain assumptions and approximations, practical solutions have been found which are of engineering value especially in the type of feed structures that are being used in this work.

Microstrip and stripline feed are the very common approaches being used to excite the endfire slotline antenna. Most of time, the feed works on the principle of microstrip to slotline transition [13]. It basically consists of a short circuit slotline which is etched on one side of the board and it is crossed at a right angle by an open-ended transmission line (stripline or microstrip line) on the opposite side as shown in Figure 5. The quarter-wave open circuit microstrip stub reflects a short circuit to the region of the slotline where they cross. This corresponds to a maximum of the current standing wave along the transmission line. Then the quarter wave short circuit slotline stub reflects an open circuit to the region

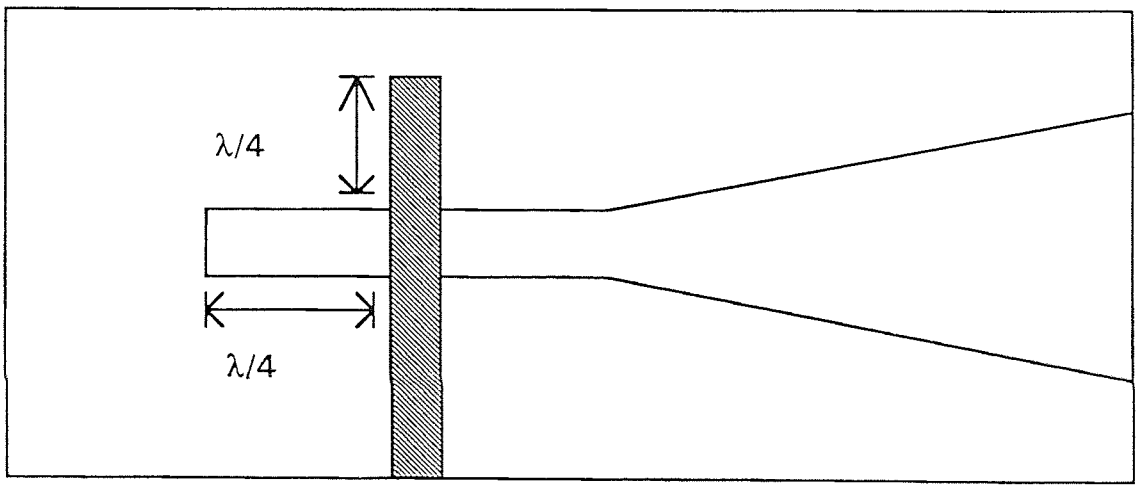

Figure 5. Transition with quarter-wave stubs on strip and slot lines

of the strip so that all the coupled waves travel off to the right along the slotline and then to the notch antenna.

The microstrip and slotline transition had been widely modeled as circuit discontinuities by quasi-static methods, equivalent waveguide models and equivalent circuit models in the past. The most common one used by Garg [14] uses a transformer model as in Figure 6. The related equation based on Figure 6 leads to a coupling ratio, n,

$$n = V(h) / V_o$$

where $V(h) = -\int_{-b/2}^{b/2} E_y(h)\,dy$

Here, b is the width of the slot region, and $E_y(h)$ is the electric field of the slotline on the outer surface of the dielectric substrate.

A similar model also proposed by Knorr [15] was backed with experimental data. These type of models do not take into account surface waves and radiation effects. But the results of these models do act as a good reference and starting point to a more rigorous and accurate solution.

A dynamic model was proposed by Yang [13] which uses the Method of Moments (MOM) to determine the current on the strip or electric field in the slot region. One important feature of this method is the modeling of two half plane-infinite lines where expansion modes are composed of piecewise-sinusoidal modes and traveling-wave and standing-wave modes.

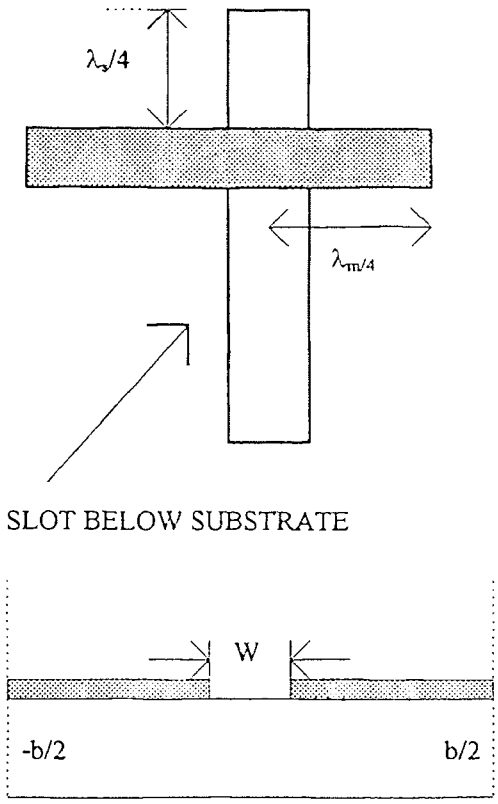

Figure 6. Top view of the microstrip-slotline transition and cross section of a slotline.

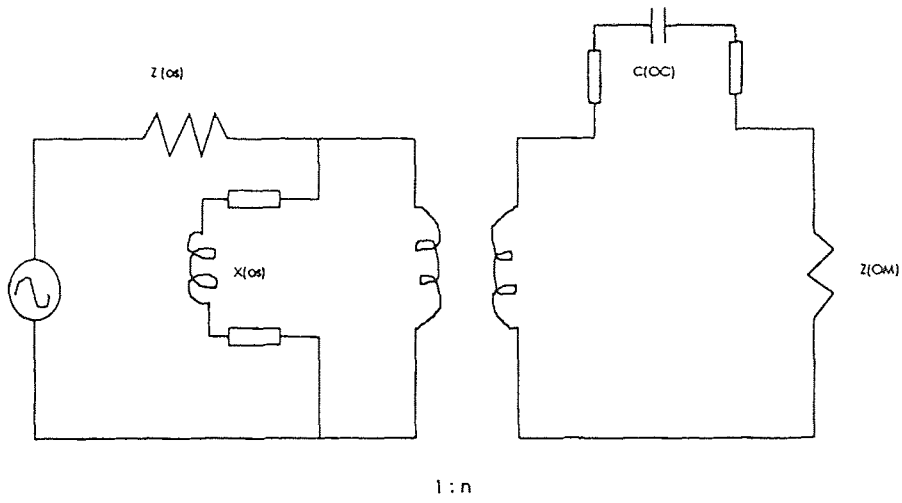

Figure 7. Equivalent transformer model of the slotline to microstrip model transition

Z[os]: Slotline impedance

Z[om]: Microstrip impedance

X[os]: Inductance of a shorted slotine

C[oc]: Capacitance of an open microstrip

2.3 Design of the antenna

Linear Taper Slot Antenna was picked because of its distinct characteristics. It can be fabricated on a very thin substrate (10mils) with very low dielectric constant like Duroid (ε_r = 2.2) and manufacturing of the antenna becomes very cost-effective. Moreover, the main design criteria was met because antenna of this type has very low sidelobes as suggested in Table 1.

The microstrip feed LTSA antenna and the stripline line version LTSA are shown in Figure 8 and Figure 9. The LTSA consists of a resonance cavity, quarter wave slot line

and a taper. The opening angle α is approximately 9.4° which produces symmetric E and H Plane beams. Length of the antenna is approximately $1.4\lambda_o$. According to Yngvesson[8] 's experimental data, these dimensions should fall within the low-side lobes curve of Zucker's " Standard Curve". The feed is consisted of 3 sections as shown in Figure 8. The input to the 1st section is 50 ohm and it is tapered down to 115 ohm which bends around (due to space limitation) and is being terminated with a quarter wavelength stub at 10.5Ghz (Center frequency of the designed antenna). The characteristic impedance of the last section is 29.6 ohm. The discontinuities between the 2nd and 3rd sections effectively are acting as tuning elements.

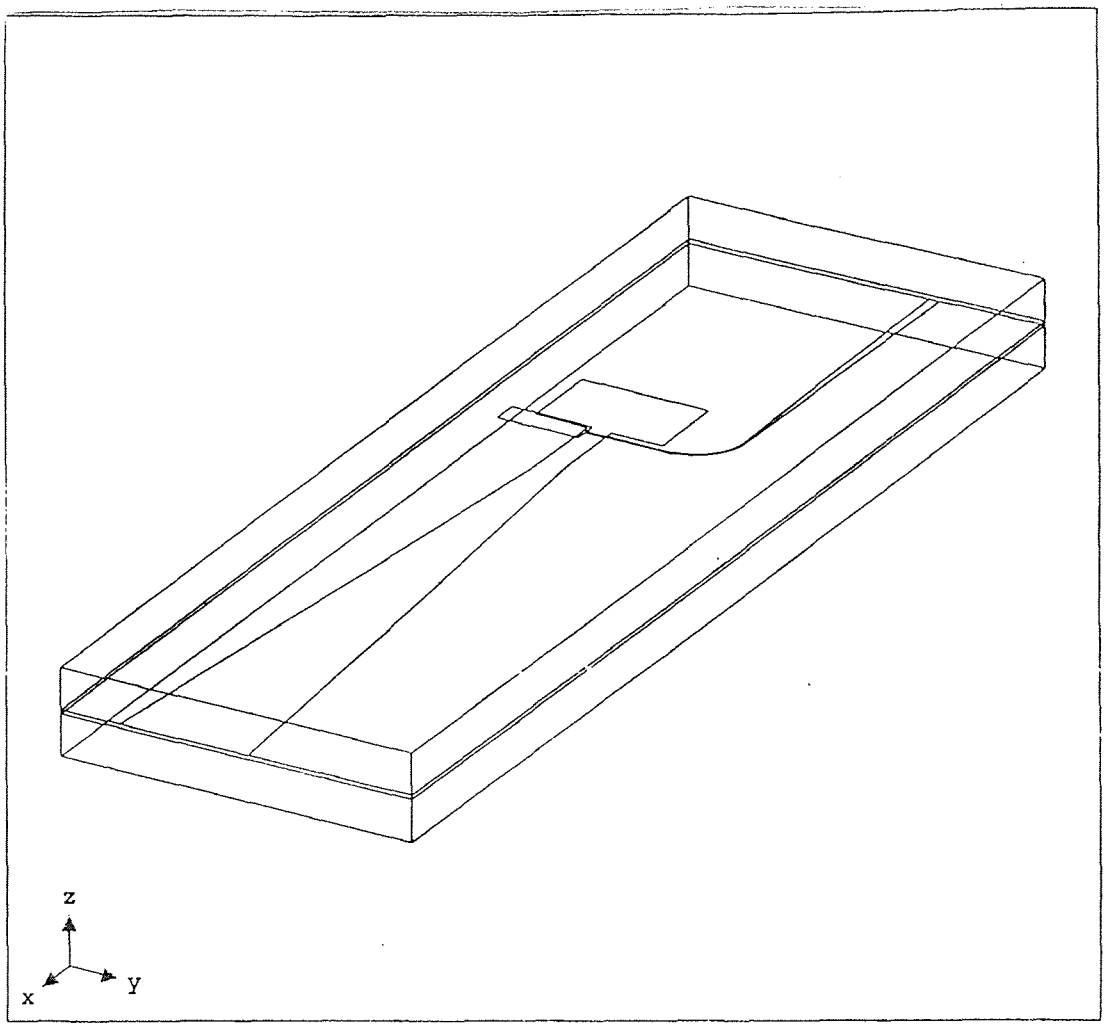

Figure 8. Microstrip feed LTSA

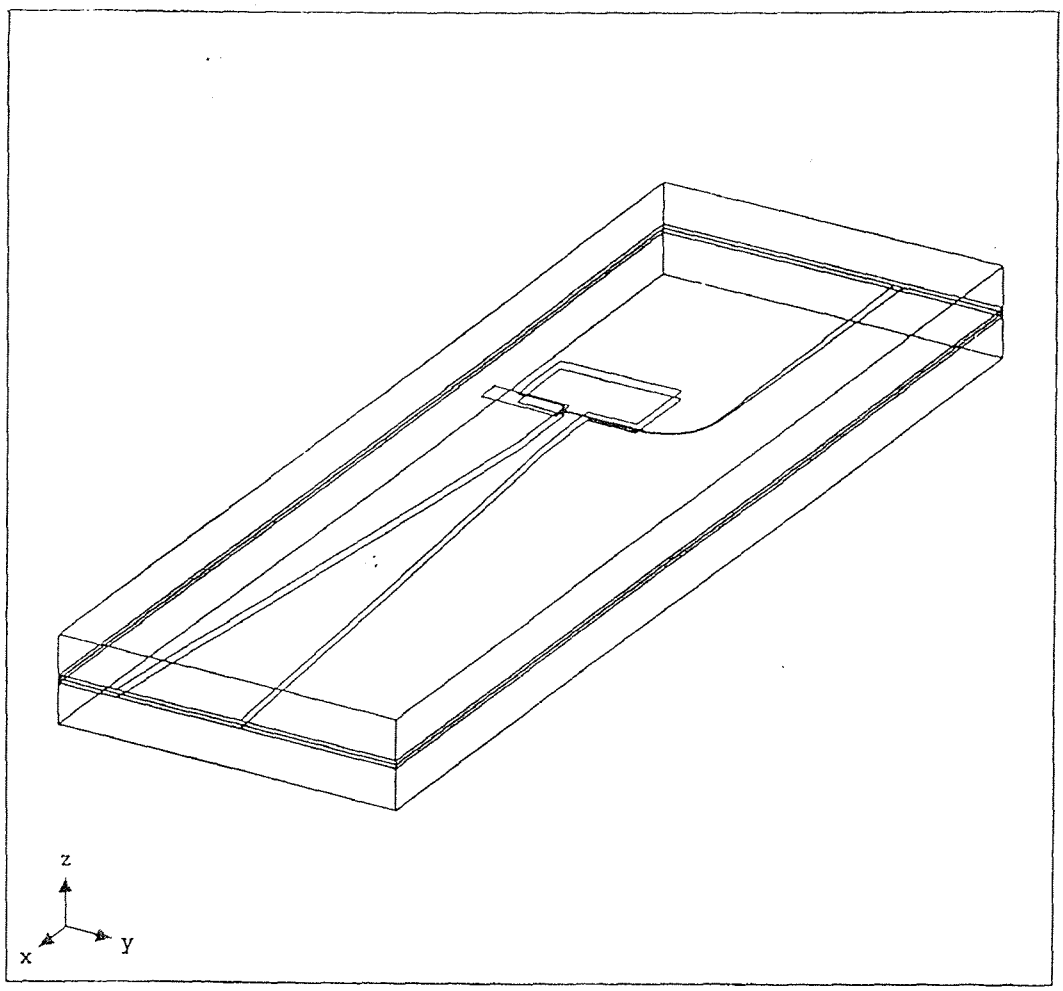

Figure 9. Stripline feed LTSA

CHAPTER 3

NUMERICAL SIMULATIONS AND RESULTS

Among available various numerical methods, the Finite Element Analysis (FEA) is chosen for specific reasons explained below.

3.1 Finite Element Analysis and High Frequency Structure Simulator (HFSS)

Three dimensional modeling of an electromagnetic field in a radiating structure requires a lot of computational time and memory. It becomes more difficult to solve if the structure dimensions are much larger than a wavelength. Finite Element Analysis approach to this kind of problems is by dividing the entire region of interest into thousands of smaller regions and to represent the field in each sub-region using a separate equation. The FEA algorithm divides such a region into a grid of nodes as shown in Figure 10 (e.g. Rectangular grid, skew grid, circular grid ....) in the 2D case or tetrahedron (a four-sided pyramid) in the 3-D case. A collection of these elements is referred to as the finite element mesh. Figure 11 shows such a mesh created using finite elements.

The value of a vector field quantity (such as the H-field or E-field) at points inside each tetrahedron is interpolated from the vertices of the tetrahedron. At each vertex, components of the field that are tangential to the three edges of the tetrahedron are stored. In addition, the vector field at the midpoint of the selected edges that is tangential to a face

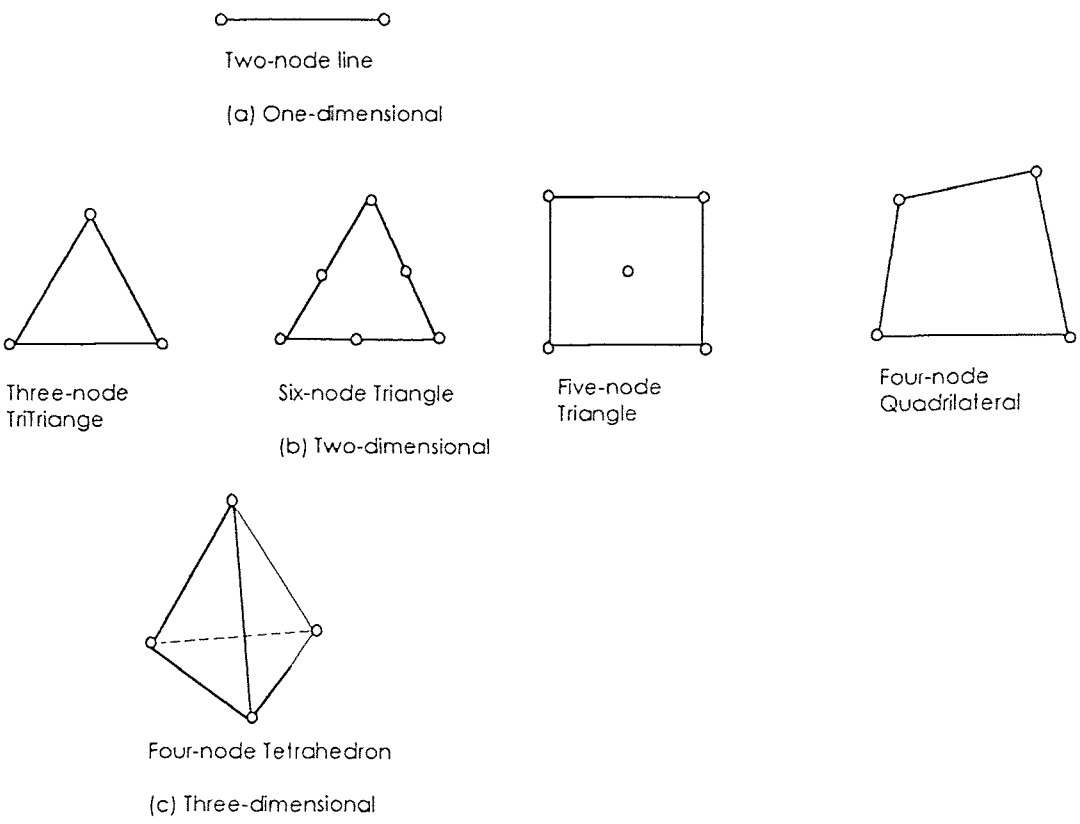

Figure 10. Typical Finite Elements

and normal to the edge is also stored. Then the field inside the tetrahedron can be interpolated from these values.

Obviously, the more the numbers of tetrahedra, the more accurate the field solution becomes. However, there is a tradeoff between size of the mesh, desired level of accuracy and the amount of available computing power. On the one hand solutions based on meshes that use thousands of tetrahedra are far more accurate than coarse meshes that have few elements. It is simply because the tetrahedral in the coarse meshes case does not

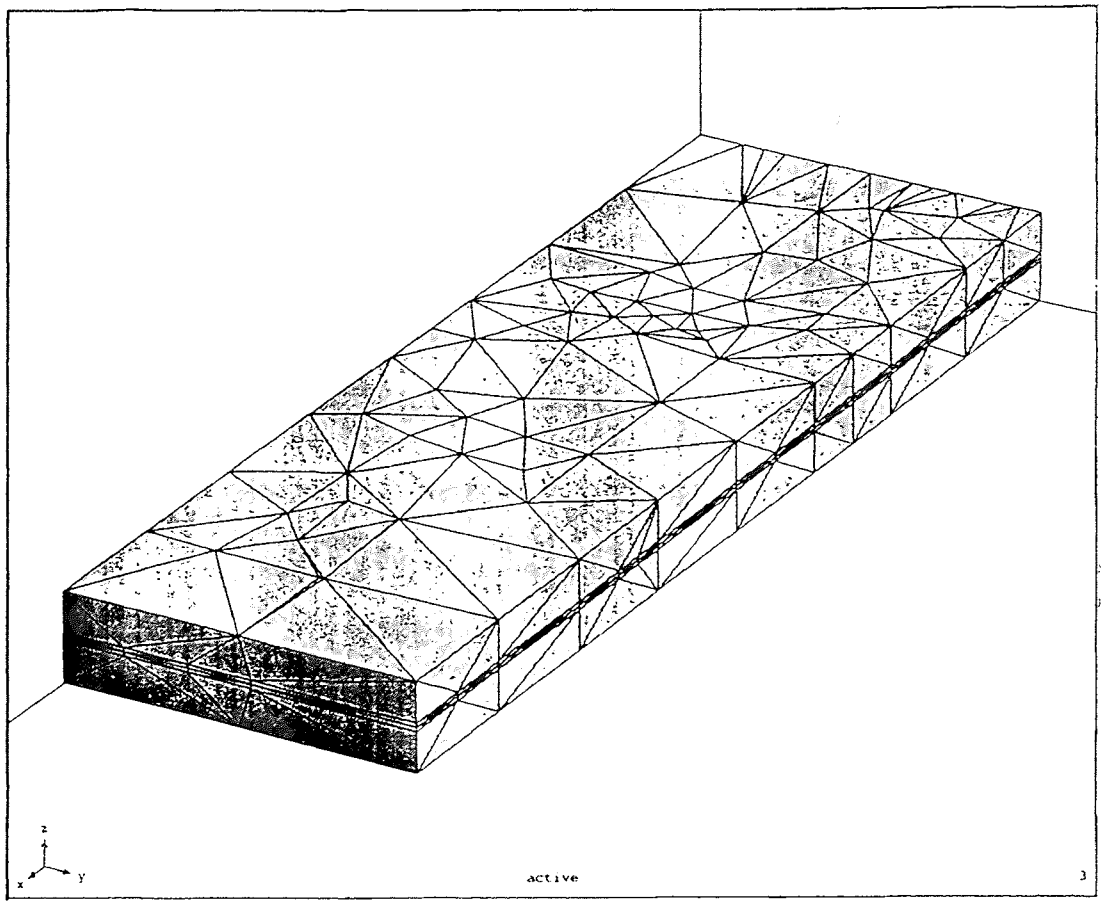

Figure 11. 3-D shaded mesh of a box containing the antenna element and lossy surface

occupy a region small enough for the field to be accurately interpolated from the nodal value. On the other hand, if the number of tetrahedra are too large, such a solution requires very large amount of computing power and time. But the accuracy may have a very small improvement over a solution with lesser tetrahedra.

High Frequency Structure Simulator (HFSS) produced by Hewlett-Packard Company is a general purpose 3-D finite element electromagnetic simulator. One of the very powerful features of HFSS is its ability in producing optimum number of tetrahedra or meshes. It uses an iterative process in which the meshes are automatically refined in critical regions. HFSS first produces a solution based on a very coarse initial mesh. Then the simulator refines the mesh in areas with high error density and generates a new solution. Limits of the amount of accuracy can also be user-defined. Since HFSS has an automatic discretization capability, users do not have to go through the tedious process of selecting the optimum grid size.

One important note on the Finite Element Method is, it uses "energy functionals " mathematical equations [16] to construct the matrix and they have the property that the energy in the system is minimized. The practical benefit of this is that the S parameters have variational properties. The S-parameters have a smaller error than the error between the actual electromagnetic fields and the approximated electromagnetic fields.

Other methods such as the Method of Moments (MOM) was not used here, because adaptive gridding feature was not built-in in the available software codes. Therefore a large portion of the structure suffers in long simulation time because of the griding requirement of the smallest part of the structure. As in our case, the feed structure

is very narrow as compared to the horn but we were forced to use very small grid size to accommodate the feed line. The resulting matrix became very big and the SUN Sparc10 Station quickly ran out of memory. We had to increase the swap space of the machine which made the computer ran even slower. The answers obtained were quite unsatisfactory. This was partly due to the over simplification of the structure to accommodate the proper grid size.

3.2 Simulations of the LTSA with HFSS

HFSS has a 3D drawing program which makes it very convenient to enter the geometry as well as modifying it when need arises. It allows almost any type of geometry (e.g. curve, elliptical ...) in both 2 and 3 dimensions and the griding is transparent to the user. There is however one limitation that all structures have to be enclosed in a box. This makes it impossible to simulate an open structure like an antenna. Fortunately, it allows lossy (impedance or resistive) boundaries which have the free space impedance (377 ohms) as shown in Figure 11 and this substitution had successfully been used in simulating an antenna in this work. Even though the frequency response reported had a slight shift, the general shape was still retained.

Various simulations of the LTSA were carried out using HFSS included:

- Simulating the antenna with 3 different substrate heights of Duroid (ε_r=2.2),

- Simulating the antenna with different locations of the feed,

- Simulating the antenna with a circular cavity instead of a rectangular cavity,

- Simulating the same antenna but with a stripline feed and an additional horn on the bottom with identical dimensions.

3.2.1 Simulating the 10 mil substrate LTSA

An adaptive analysis yielded close to 6,000 tetrahedra in order to reach a converged solution. This takes approximate 1 hour and 15 minutes on the HP 700/715 Workstation equipped with 80 Mb RAM. Plot of the magnitude and phase of the return loss, $|S_{11}|$ around 10.55 Ghz in Figure 11 and is also compared to the measured data of the antenna obtained from the HP 8510C in Figure 13. It shows the simulated data has a slight shift to the right but the general trend follows very closely. The slight shift could be due to a combination of the error introduced by the free space impedance boundary, the uneven surface on the substrate and the connector itself. The comparisons provided us with confidence that HFSS is an accurate and a valuable tool to apply trial and error approach before more antennas are fabricated.

3.2.2 Comparison of 20 mil, 15.5 mil, 10 mil Duriod substrate of the LTSA

Figure 14 shows the comparisons of $|S_{11}|$ of all 3 different thicknesses of the substrate. The antenna with 10 mil thickness has the best response, with > 25 dB return loss. The thicker the substrate, the less is the return loss. The resonant frequency also shifts towards the left of the spectrum with the increase of substrate thickness. The decrease in return

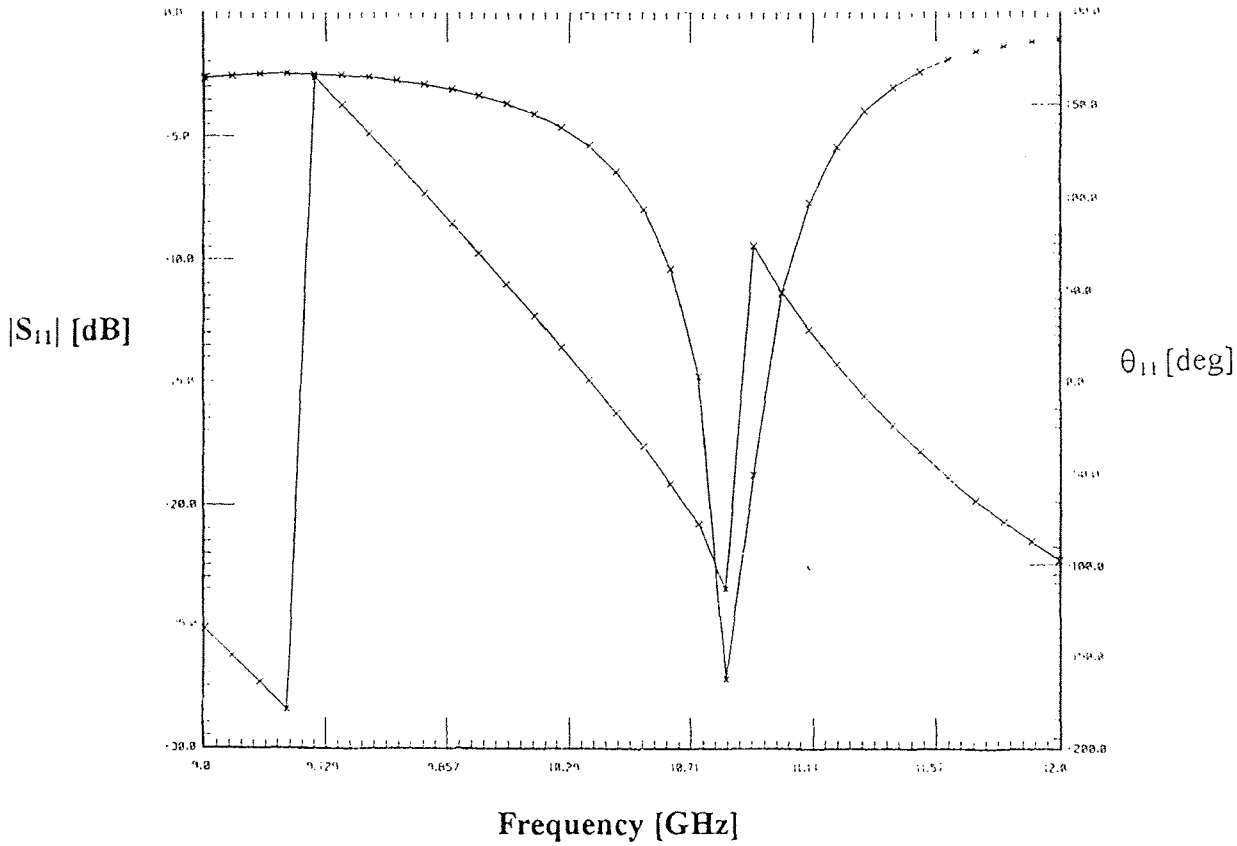

Figure 12. Simulated S_{11} (both magnitude and phase) of the microstrip LTSA element.

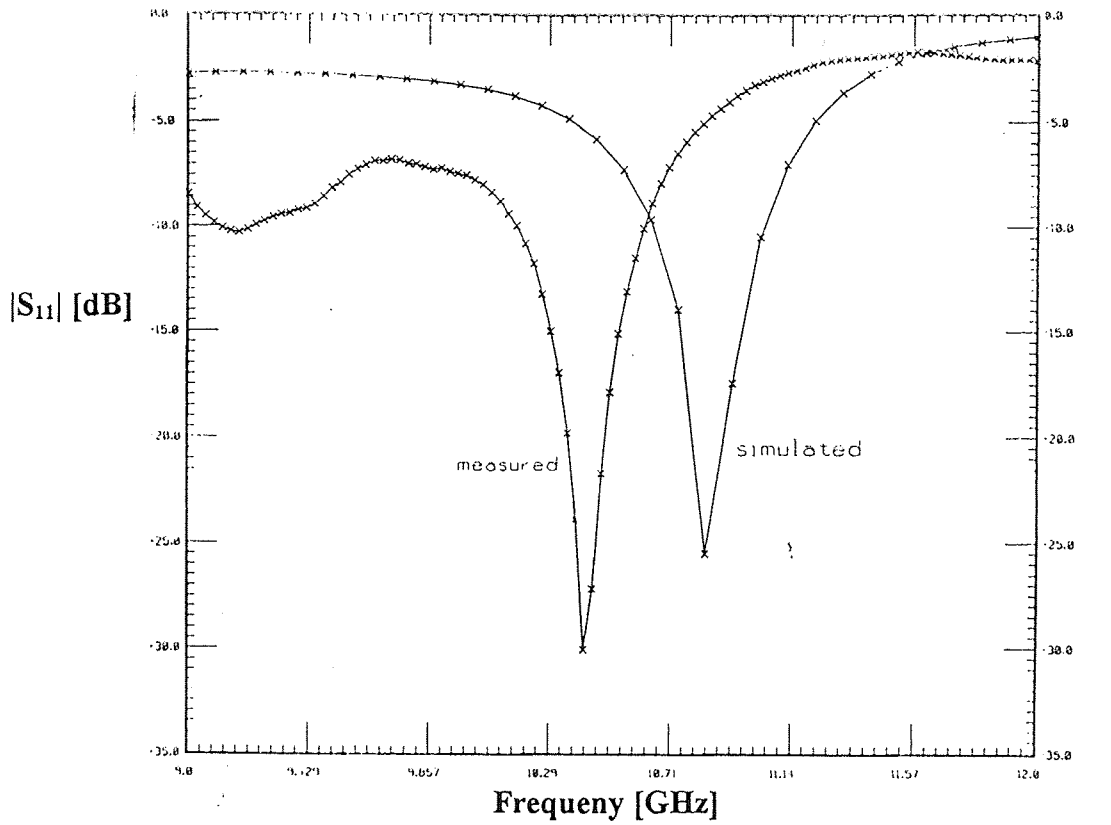

Figure 13. Measured $|S_{11}|$ versus simulated $|S_{11}|$ of the microstrip feed LTSA versus frequency.

loss is due to the decrease in coupling between the microstrip feed and the slotline antenna. This ultimately changes the reactance between the microstrip and the slotline which causes the resonant frequency to shift. Since the optimum response is observed for 10 mils then the remaining simulations are restricted to 10 mils thick substrate which is commonly available from commercial sources.

3.2.3 Comparison of the rectangular and the circular cavity

The diameter of the circular cavity in Figure 15 is chosen to be identical to the width of the rectangular cavity of Figure 8. The reason for picking this width is to ensure that there is a comparable solution, which can be used to observe the variation. The return loss $|S_{11}|$ for both geometries is plotted in Figure 16. The rectangular cavity has a sharper response in return loss (< -25 dB) than the circular cavity. But the bandwidth is slightly narrower than the circular cavity. This is consistent with the gain-bandwidth tradeoff theory [9]. The circular cavity response curve also shifts to a lower frequency. Observations of the phase of S_{11} curve show the transition through 0° phase is in consistence with the dip at the resonance in $|S_{11}|$ curve as can be seen in Figure 12.

3.2.4 Optimization of the feed location of the rectangular cavity

As for the feed location of the rectangular cavity, with respect to the slotline various feed positions were studied. One is the original feed postion in which the microstrip stub

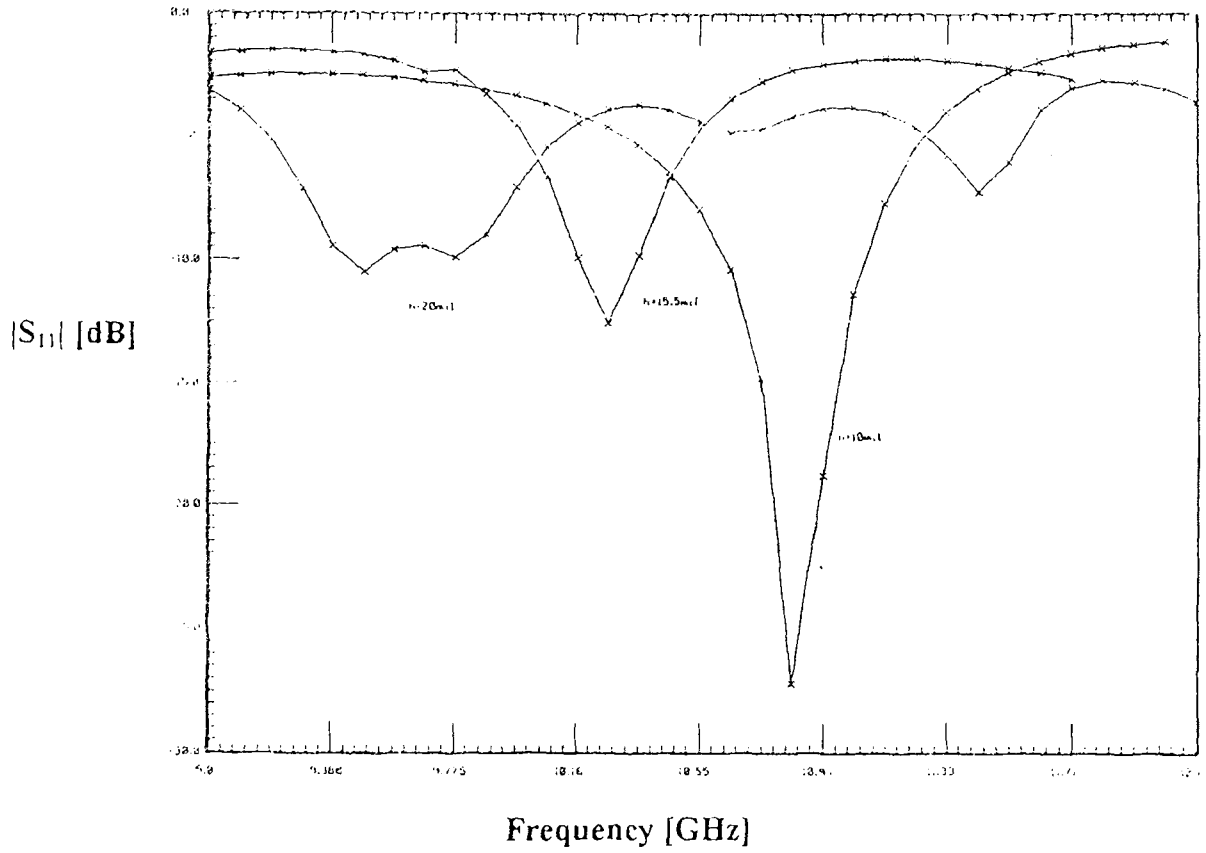

Figure 14. Variation of $|S_{11}|$ versus frequency for three different substrate thicknesses.

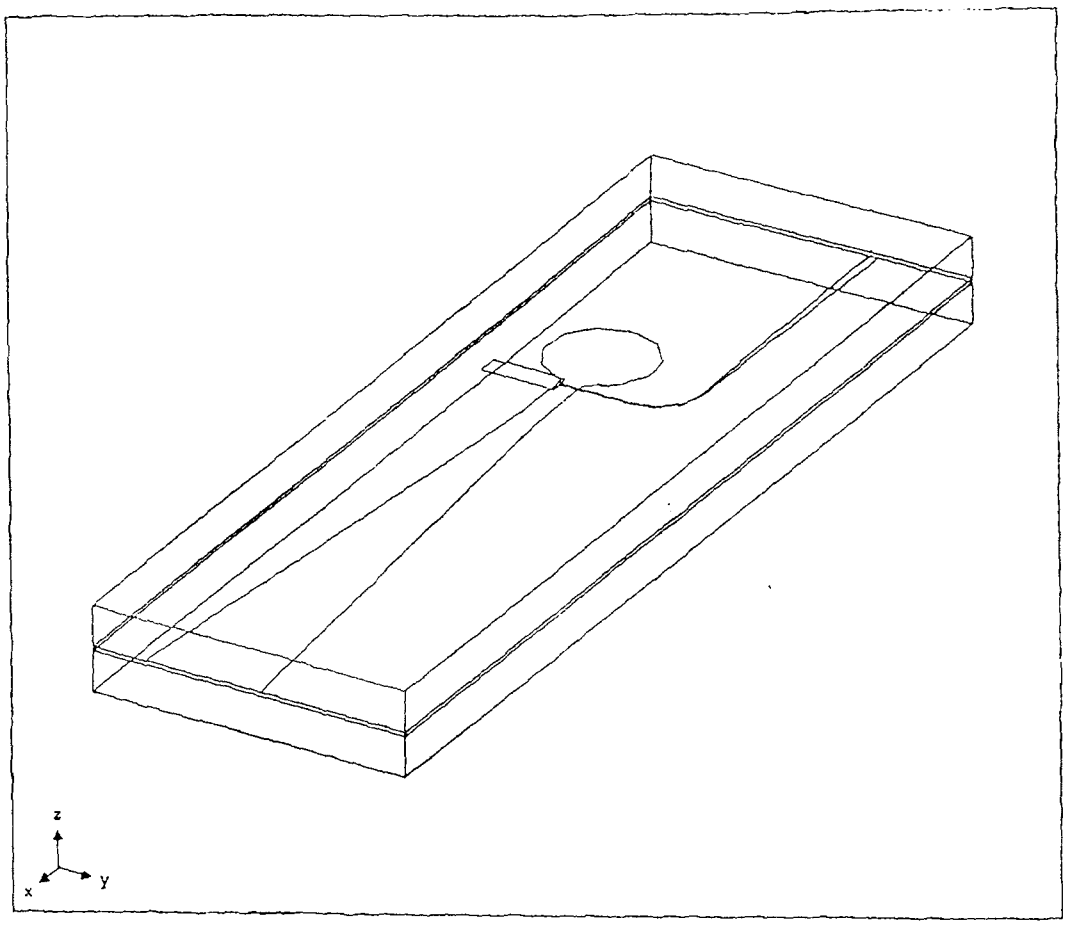

Figure 15. LTSA with a circular cavity

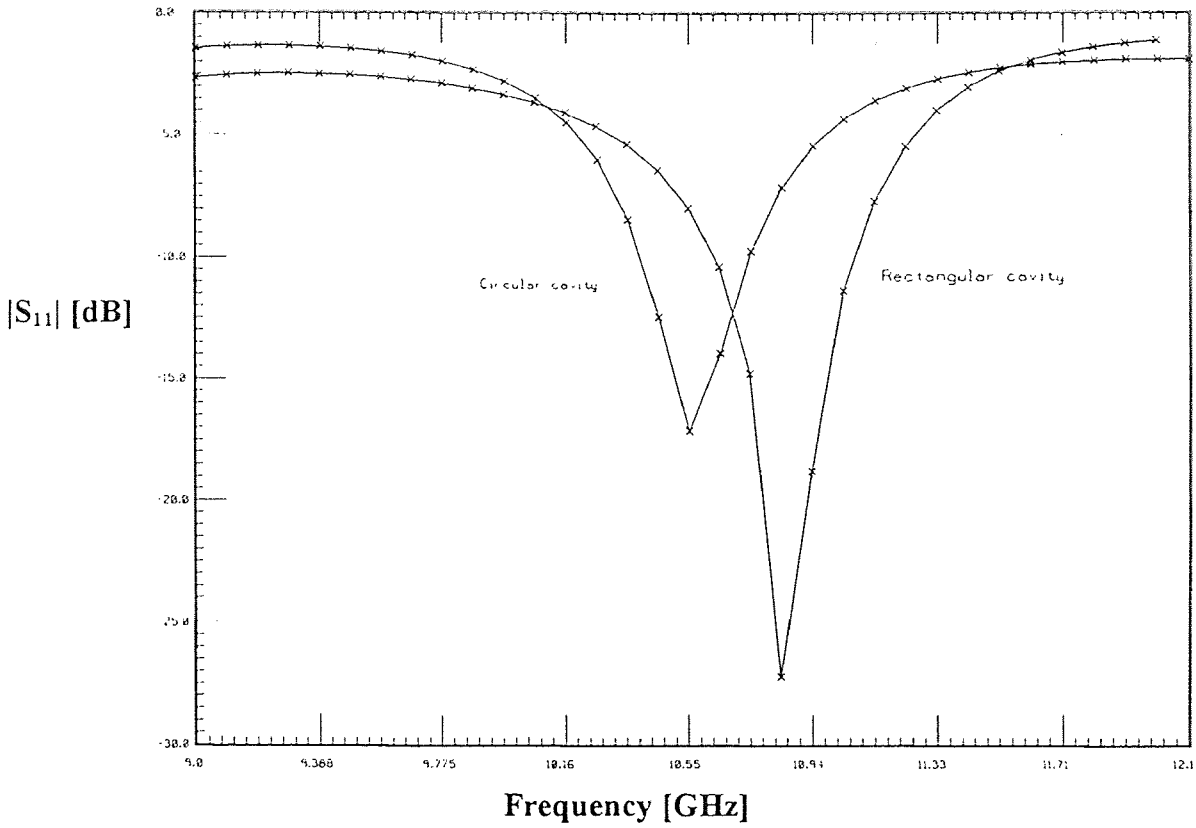

Figure 16. Comparison of an
cavities: $|S_{11}|$ variations versus frequency. The physical dimensions of these antennas are shown in Figure. 17.

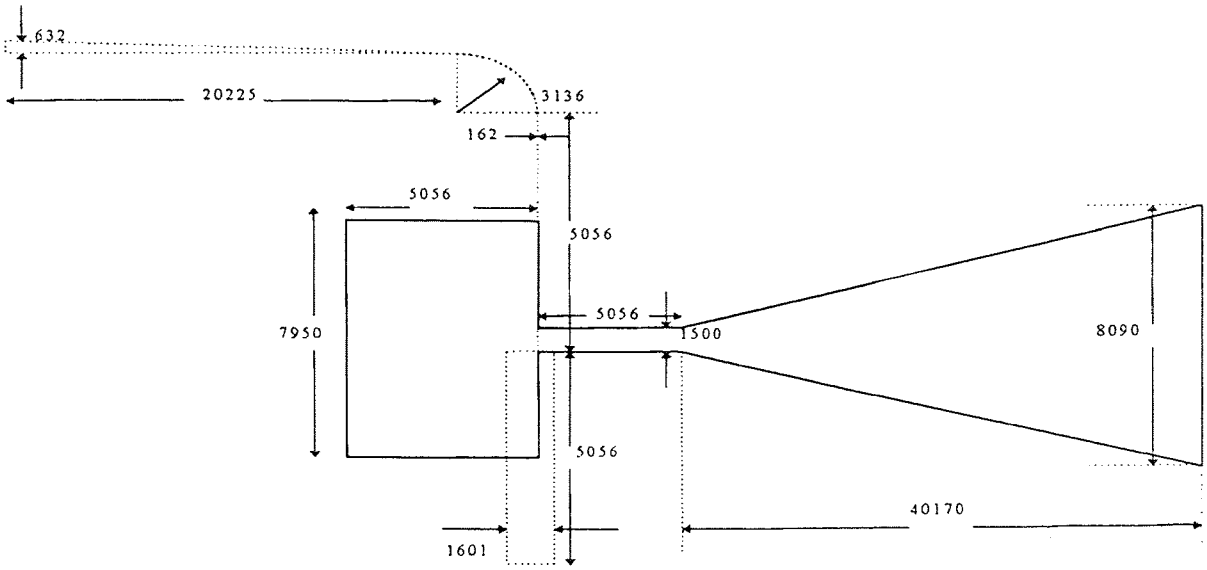

(a) The microstrp feed LTSA with rectangular cavity.

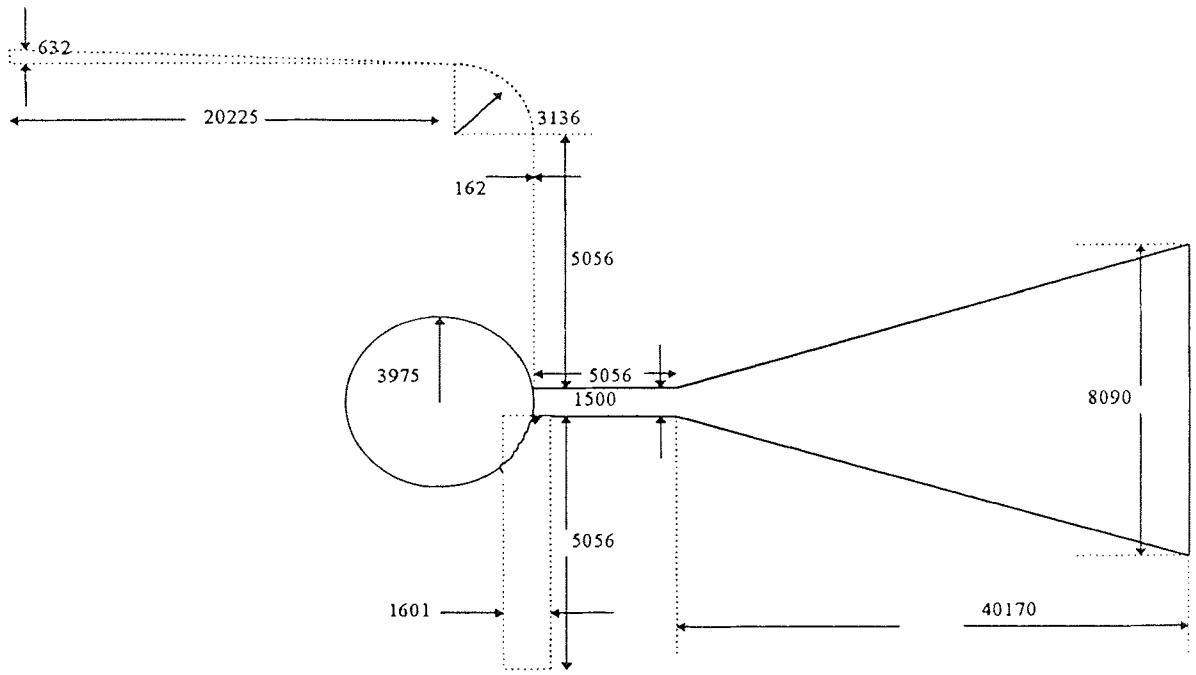

(b) The microstrip feed LTSA with circular cavity.

Figure 17. Physical dimensions of LTSA elements. All dimensions are given in microns.

location exactly overlaps the slotline in a quarter wave manner. The other one is having the microstrip offset slightly to a width less than quarter-wave overlap with the base of the strip rests in the middle of the slotline as indicated in Figure 18. The comparisons for such two feed arrangements are plotted in Figure 18. The $|S_{11}|$ changes from < -25dB to < -16dB, and the bandwidth, however, increases slightly, for the middle position of Figure 18.

3.2.5 Optimization of the feed location of the circular cavity

Variations have also been applied for the circular cavity elements which are identical to the rectangular case,results for the original feed and middle feed locations. Figure 20 and Figure 21. However, the behavior of feed location variations in circular cavity cases are quite different. As far as the return loss $|S_{11}|$ is concerned as seen in Figure 21, the middle feed case is worse that the original feed which is consistent with the rectangular cavity case. But the resonant frequency shifted quite a bit in between the feed locations, resonance frequency shifted to the right of the spectrum for the middle feed as compared to the original feed case.

3.2.6. Simulation of the rectangular cavity LTSA with stripline feed

The LTSA element backed with a rectangular cavity excited by microstrip line (Figure 9) is now covered by an additional symmetrical notch antenna. The resulted antenna is shown in Figure 9 and is now excited by an equivalent strip line. The simulated results are shown in Figure 22. The return loss, $|S_{11}|$ has now dropped to -8.5 dB and the phase deviation

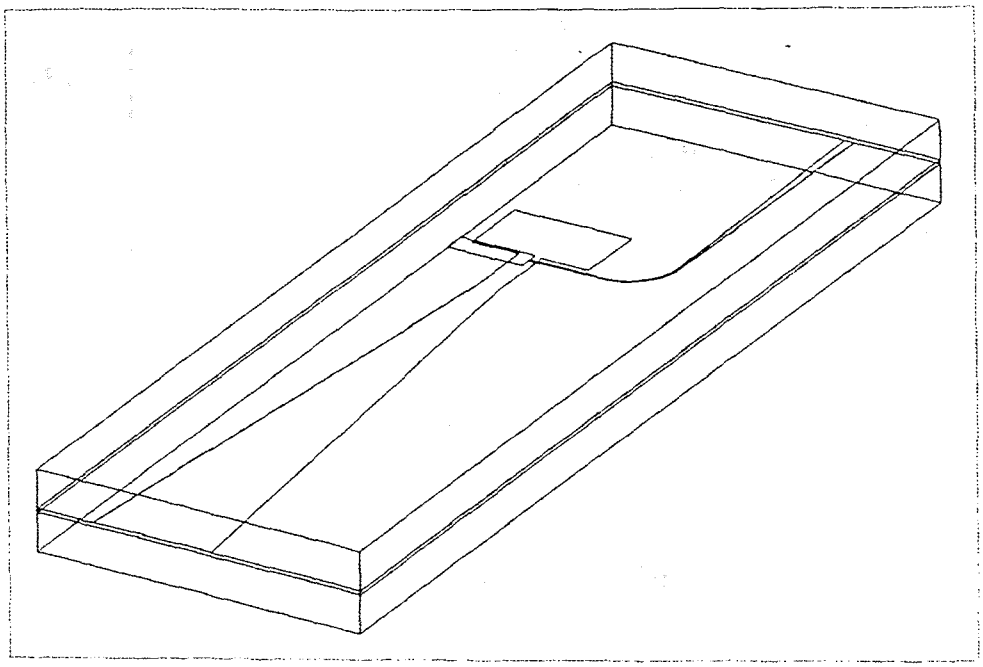

Figure 18. Microstrip feed for the LTSA element when the base of the stub is in the middle position within the slotline backed by the rectangular cavity.

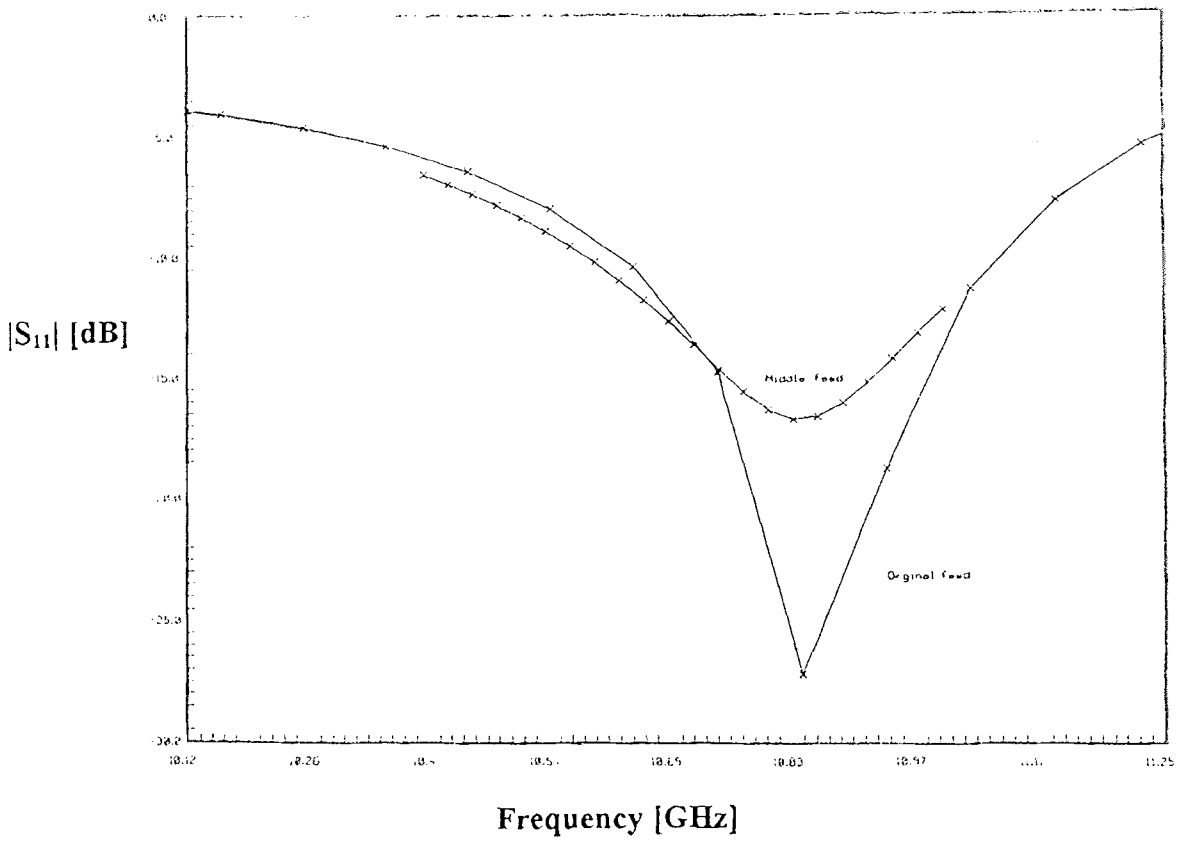

Figure 19. Variation of $|S_{11}|$ versus frequency for two different feed arrangements as shown in Figure 18 (middle position) and Figure 8 (original position) for the rectangular cavity.

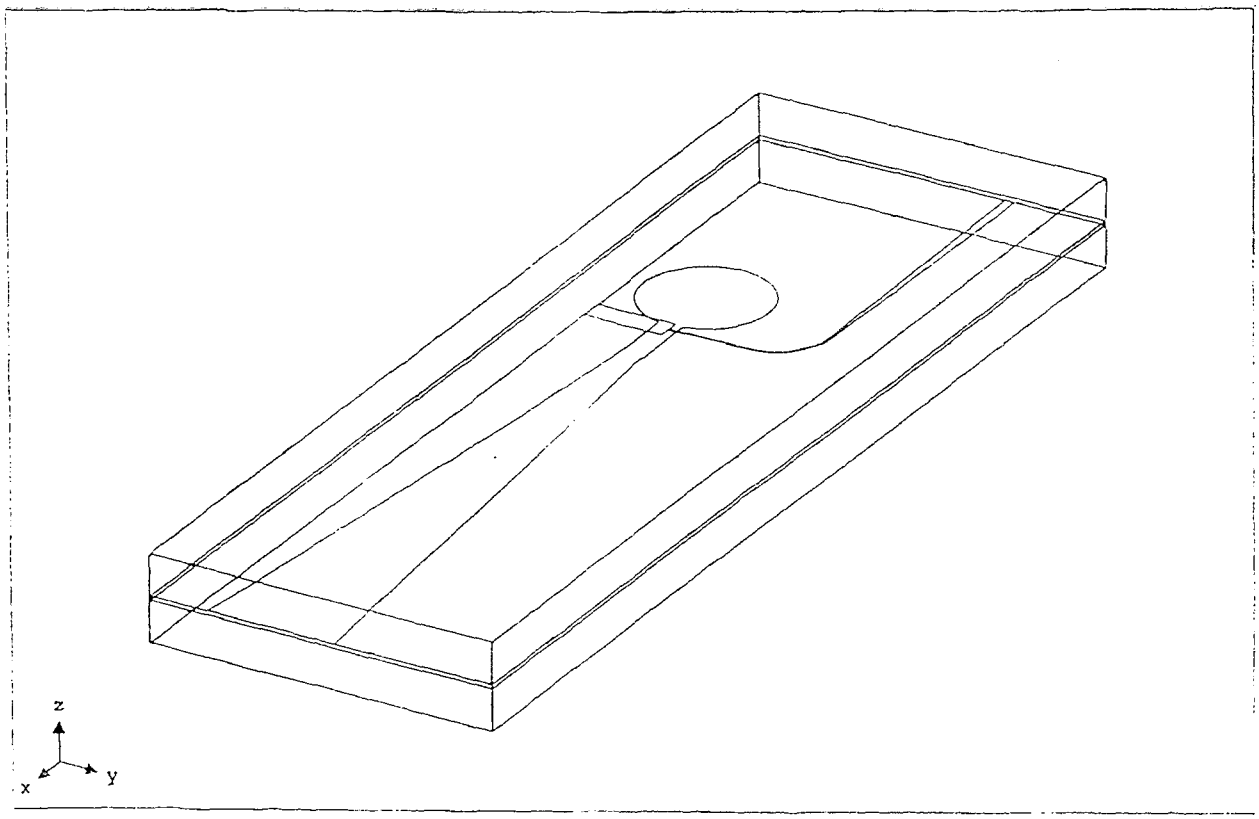

Figure 20. Excitation of the LTSA antenna element with the stub base located in the middle of the slot for the circular cavity.

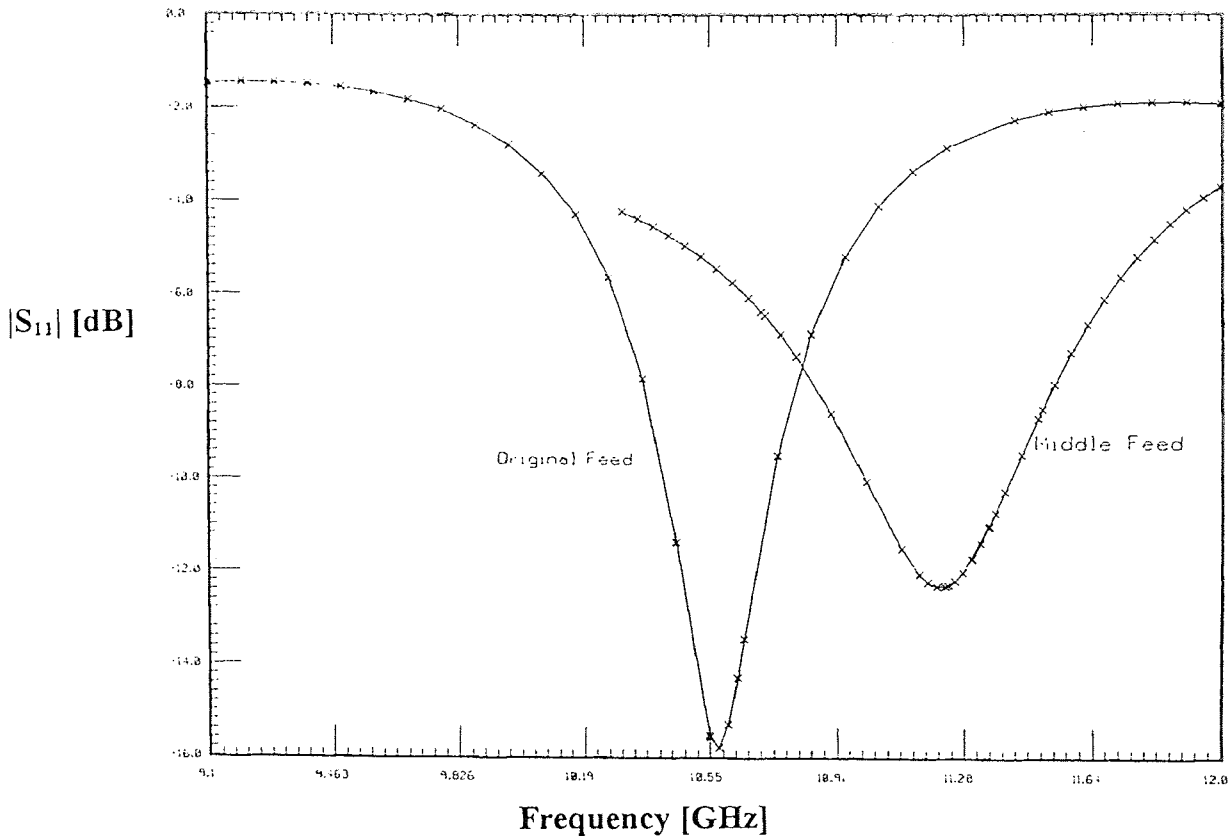

Figure 21. Comparison of $|S_{11}|$ of the original feed (Figure 15) and the middle feed (Figure 20) positions with respect to the slot backed by a circular cavity excited by the microstrip line.

around resonance does not show a full swing as compared to previous results.

3.2.7. Simulation of the circular cavity LTSA with stripline feed

The response due to an LTSA element backed with a circular cavity excited by a strip line yielded -26 dB at resonance condition (Figure 23). The phase response was also quite consistent with the resonance condition exhibiting a large swing. However, the resultant bandwidth has been reduced substantially compared to the microstrip excited case.

3.2.8 Current density variation along the feed line

The feed line structure for the LTSA element consists of a stub connected through the tapered line (impedance transformer) to the source. The quarterwave stub is designed so that the current maximum occurs at the base. However due to loading effects, the entire structure is coupled to the feed line and the position of the current maximum shifts along the line. Typical results are shown in Figure 24(a) where the current density maximum is located quite a distance away from the base of the stub.

The loading effects can be overcome by shifting the feed location to the right which overlaps the slotine by half of the slotline's width. The maximum current density occurs at the loaction by the end of the stub as it was orginally designed for.

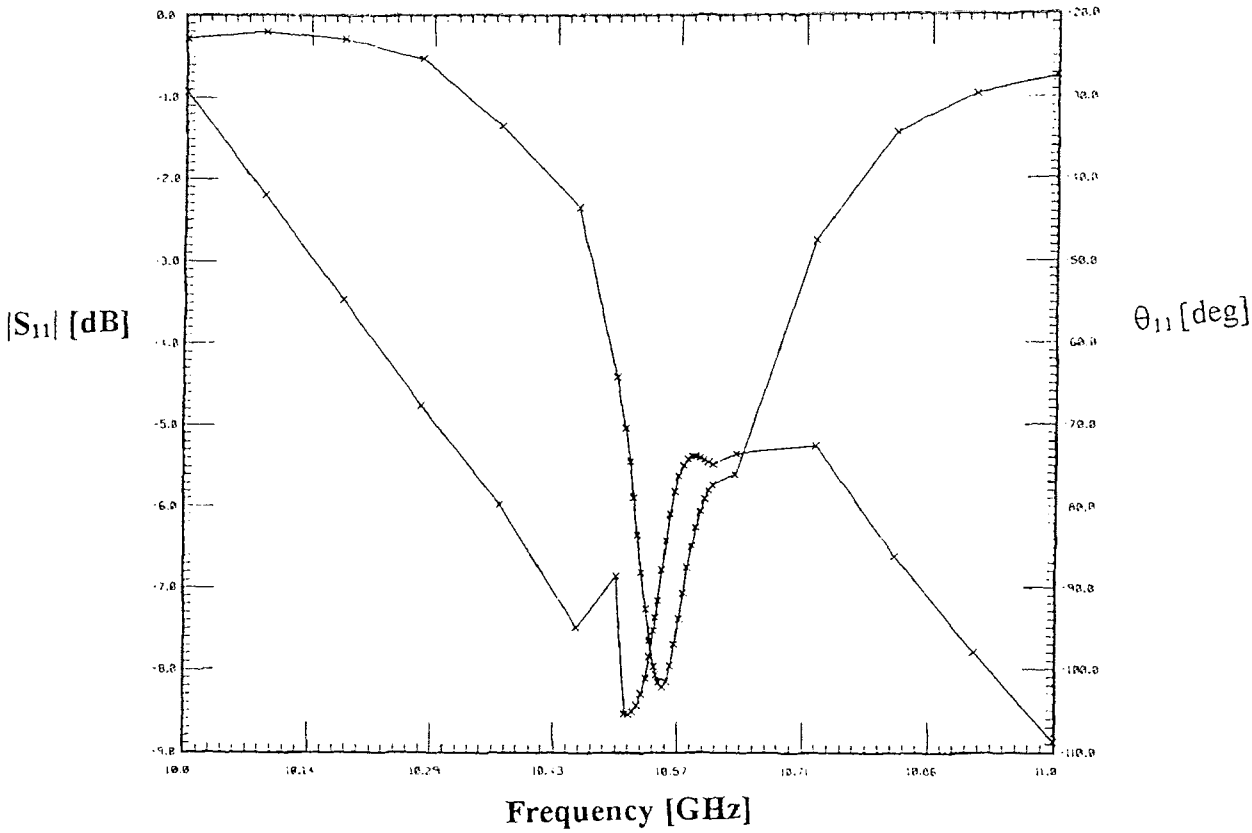

Figure 22. S_{11} variation versus frequency for a rectangular cavity LTSA with a strip line excitation.

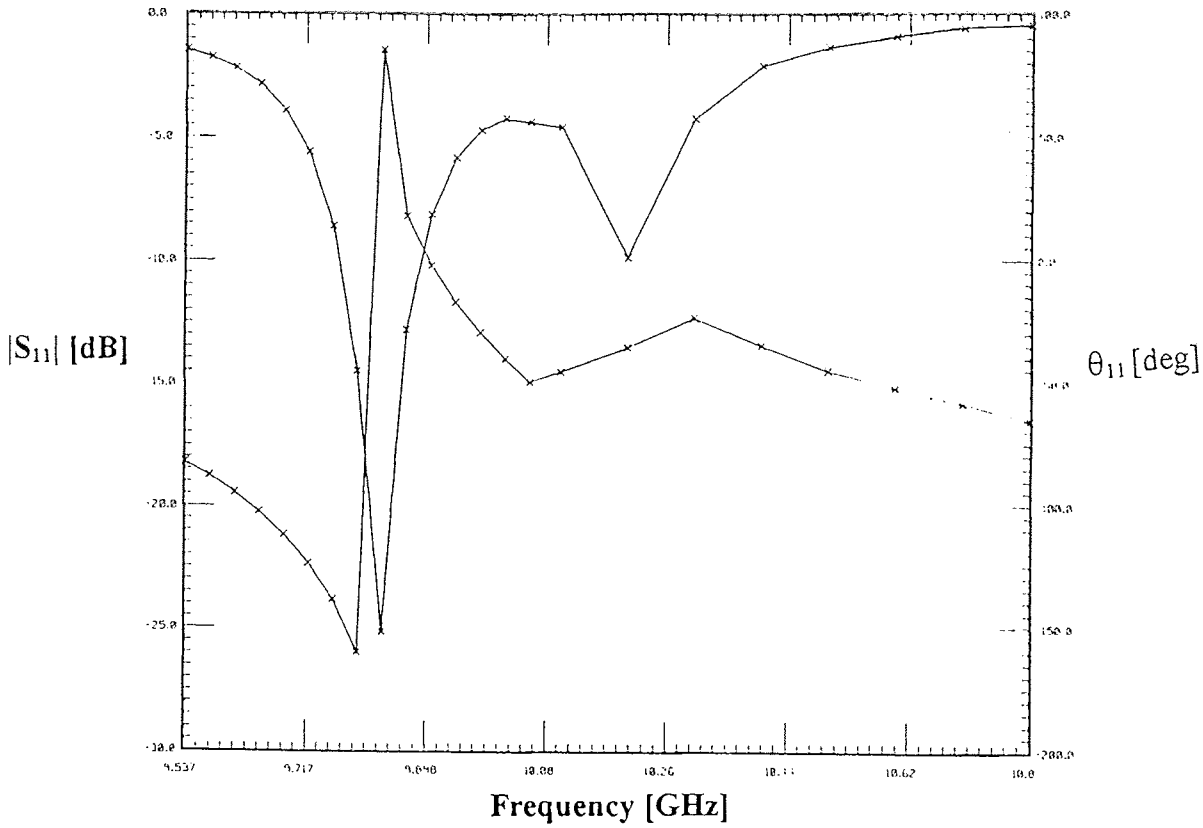

Figure 23. S_{11} variation versus frequency for a circular cavity LTSA with a strip line excitation.

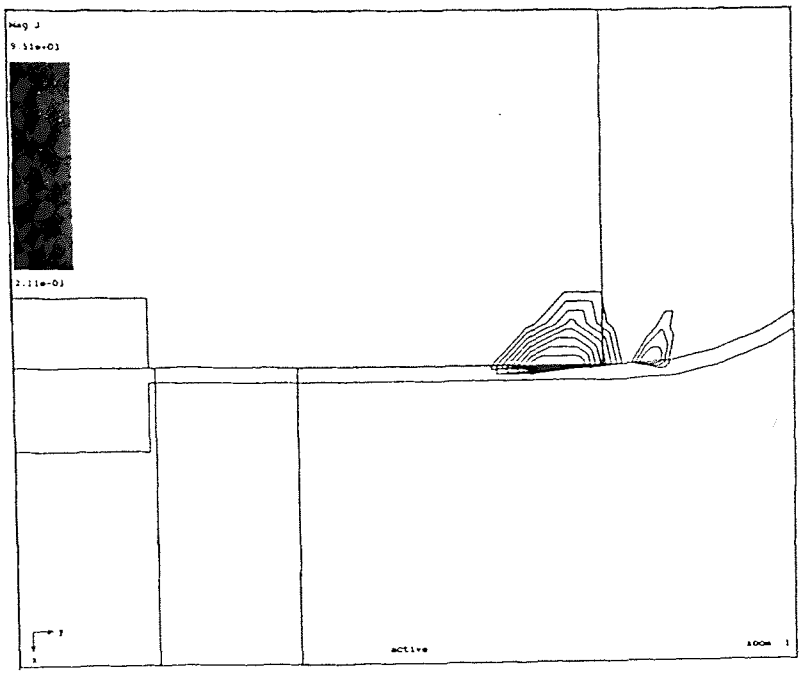

Figure 24(a). Current distribution of the feed line for the rectangular cavity backed LTSA with the original feed position.

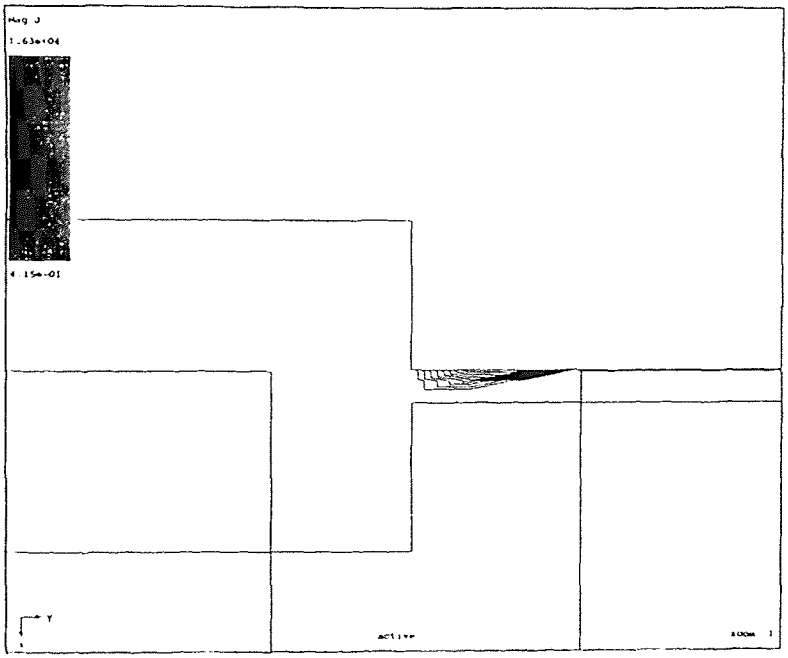

Figure 24(b). Current distribution of the feed line of the rectangular cavity backed LTSA with the middle feed position.

CHAPTER 4

CONCLUSIONS

The CAD study of the Linear Tapered Slot Antenna (LTSA) revealed that such an antenna has many parameters that can be optimized for its use in frequency scanning arrays. Comparison of simulated results with the measured data confirms the validity of the usage of the computer code based on finite elements such as HFSS.

Among the various optimization parameters such as substrate thickness, taper angle, position of the feed line with respect to the slotline and the size of the rectangular cavity, it is possible to add other physical variables dictated by the chosen geometry.

The feed line consisting of a $\lambda/4$ stub and tapered impedance transformer is designed to couple efficiently to the slotline based on the current maximum at the base of the stub. During numerical studies it was observed that the current maximum location could shift because of the field interactions between the feed line and the rest of the radiating structure. The current maximum could be shifted back to the slotline region by varying the feed position which may help to improve the performance. Furthermore, the rectangular cavity in LTSA could be modified to a circular one, which could improve the bandwidth. Further study has to be conducted on what kind of modes will be excited when the circular cavity is introduced and their effects on the overall performance.

REFERENCES

[1] J. W. Mink and F. K. Schwering, "Intergrated Antennas" Section 12.3, Handbook of Microwave Optical Components, Wiley-Interscience, 1990.

[2] N. A. Begovich, "Frequency Scanning," Ch. 2, R.C. Hansen "Microwave Scanning Antennas," Vol III, Academic Press, 1966.

[3] James S. Ajioka (Ed.), "Frequency Scanning Antenna" Ch. 19, *Antenna Engineering Handbook*, McGraw Hill, 1984.

[4] Raymond S. Pengelly, "MMIC Foundry Models using Standard CAD" Compact Software Seminar, 1989.

[5] K. Chang (Ed.), *Handbook of Microwave and Optical Components, Microwave and Antenna Components*, Vol. I, John Wiley & Sons, 1990.

[6] P. J. Gibson, "The Vivaldi Aerial" Digest of 9th European Microwave Conference, pp. 120-124, Brighton, U.K., 1979.

[7] S.N. Prasad and S. Mahapatra, "A New MIC Slotine Aerial," IEEE Transactions on Antenna and Propagations, Vol. AP-31 No. 3 pp. 525-527, 1983.

[8] K.S. Yngvesson, D.H. Schaubert, T.L. Korzeniowski, E.L. Kollberg, T. Thungren and J. Johansson, "Endfire Tapered Slot Antennas on Dielectric Substrates," IEEE Transctions on Antennas and Propagation, Vol. AP-33 No. 12, pp. 1392-1400, 1985.

[9] F. J. Zucker, "Surface Wave Antennas and Surface-Wave Excited Arrays," Chapter 12, *Antenna Engineering Handbook*, McGraw Hill, 1984.

[10] R. Janaswamy and D. H. Schaubert"Analysis of the Tapered Slot Antenna," IEEE Transactions on Antenna and Propagation, Vol. AP-35, No 9, pp. 1058-1065, 1987.

[11] R. Carrel, "The Charateristic Impedance of the Two Infinite Cones of Arbitrary Cross-section," IRE Transactions on Antennas and Propagation, pp. 197-201, 1958.

[12] S. Kobayashi, R. Mittra and R. Lampe, "Dielectric Tapered Rod Antennas for Millimeter-Wave Applications," IEEE Transactions on Antennas and Propagation, Vol. AP-30, No 1, pp. 286-293, 1982.

[13] H. Y. Yang and N. G. Alexopoulos, " A Dynamic Model for Microstrip-Slotline Transition and Related Structures, " IEEE Transaction on Microwave Theory and Techniques, Vol 36, No 2, pp. 286-293, 1988.

[14] K.G. Gupta, R. Garg, and I. J. Bahl, *Microstrip Lines on Slotines*, Dedham, MA, Artech House, 1979.

[15] J. B. Knorr, " Slot-line transitions, " IEEE Transations on Microwave Theory and Techniques, Vol. MTT-22, pp. 548-554, 1974.

[16] HP High-Frequency CAE Design Forum, Hewlett-Packard Company, 1993.